1-1-2006

Electrochemical studies of hexacoordinate hemoglobins

Puspita Halder
Iowa State University

Electrochemical studies of hexacoordinate hemoglobins

by

Puspita Halder

A thesis submitted to the graduate faculty

in partial fulfillment of the requirements for the degree of

MASTER OF SCIENCE

Major: Biochemistry

Program of Study Committee:
Mark Hargrove, Major Professor
Alan Dispirito
Hans Stauffer

Iowa State University

Ames, Iowa

2006

Graduate College

Iowa State University

This is to certify that the master's thesis of

Puspita Halder

has met the thesis requirements of Iowa State University

Signatures have been redacted for privacy

To My Parents

TABLE OF CONTENTS

LIST OF FIGURES

LIST OF TABLES

ABSTRACT

Present in most organisms, hexacoordinate hemoglobins (hxHbs) are proteins that have evolved the capacity for reversible *bis*-histidyl heme coordination. The heme prosthetic group of heme proteins enables diverse protein functionality, such as electron transfer, redox reactions, ligand transport, and enzymatic catalysis. The reactivity of heme is greatly affected by its coordination and the non-covalent chemical environment imposed by its connate protein and also by the nature of ligands present at the protein active center. Of considerable interest is how the hxHb globin fold achieves reversible intramolecular coordination while still enabling high-affinity binding of oxygen, nitric oxide, and other small ligands.

Here this property is explored by examining the role of the protein matrix on coordination behavior in a group of hxHbs from animals, plants, and bacteria. This is done with a set of experiments measuring the reduction potentials of each wild type hxHb; its corresponding mutant protein where the reversibly bound histidine (the distal His) has been replaced with a non-coordinating side chain; and the mutant proteins saturated with exogenous imidazole, enable to assess the effects of the protein matrices on histidine coordination. The results show that the globin moiety of hxHb demonstrates flexible regulation of hexacoordination. The effect of ligand binding to the ferrous form of hxHbs is also studied by measuring their redox potentials in presence and absence of CO. The outcome of this study could be utilized to evaluate their potential physiological function in the context of ligand binding.

CHAPTER 1: INTRODUCTION

Background

Hemoglobins (Hbs) are a class of proteins long associated with storage and transport of oxygen in mammalian systems. They are generally described as proteins that bind to heme iron protoporphyrin IX (heme b) by using a highly conserved alpha-helical globin fold (3-over-3 fold). The heme iron atom can exist in two different oxidation states: ferrous (Fe^{2+}) or ferric (Fe^{3+}) and can adopt an octahedral geometry by satisfying its six co-ordination sites. Heme pyrrole nitrogens occupy four equatorial binding sites; one of the axial sites is bonded through the nitrogen atom of histidine side chain (proximal histidine) of the protein backbone which is invariant in the Hb super-family. The remaining axial site stays vacant in proteins where the Fe is penta-coordinate such as myoglobin in absence of exogenous ligands. The gaseous ligands like CO, O_2, and NO can bind to the sixth site reversibly for the pentacoordinate hemoglobins.

In addition to the well known hemoglobins and myoglobin, a third type of globin has recently been discovered. In vertebrates, they are predominantly expressed in the brain, nerve tissues, fibroblasts and related cell types. This new class of proteins is known as hexacoordinate hemoglobins (hxHbs) (*1, 2*), examples are neuroglobin (Ngb) and cytoglobin (Cgb). HxHbs are also found in plants and are known as non-symbiotic hemoglobins (nsHbs) e.g.; rice hemoglobin (RHb1) (*3*). The common characteristic feature of all these hxHbs is that the heme iron is coordinated by another histidine side chain in the distal site in both oxidation states, while keeping the traditional coordination behavior exhibited by the pentacoordinate hemoglobins. This hexa-coordinating side chain exerts

significant influences on ligand binding for these proteins. This is the reason for showing complicated ligand binding reactions for hxHbs compared to simple bimolecular reaction observed with traditional pentacoordinate hemoglobins (*1, 4*). However, they share the similar 3-over-3 α helical sandwiched structures which are found to be conserved in the globin family. Recent studies revealed another hxHb, *Synechocystis* SP. PCC 6803 (*Syn*Hb), found in cyanobacteria, which is a member of the truncated hemoglobin (trHb) family (*5*). The trHb proteins are typically 20-30 amino acid residues shorter than vertebrate Hbs and their globin fold consists of 2-over-2- α helical structure (*6*).

The discovery of different types of hxHbs has opened up a new field of scientific understanding in the hemoglobin family, but their roles are still under investigation. The physiological functions of nsHbs and other hxHbs have not been fully explored yet (*7-11*). However, there are growing evidences that these proteins might play a crucial role in oxygen storage and transport, detoxification of NO and other reactive oxygen species, sensing O_2 and other small molecular ligands, and involvement in other intracellular signaling pathways (*12*). It has also been proposed that Ngb and Cgb can act as terminal oxidases to produce NAD^+ for supporting the glycolysis cycle and ATP production under hypoxic condition (*13*).

Heme Proteins and redox potentials

Looking back to the traditional biological functions of hemeproteins, we can categorize them into three different classes: transport of electrons (e.g., cytochrome *b5*, cytochrome *c*), transport and storage of oxygen (e.g., hemoglobin, myoglobin), and catalysis of redox reactions (e.g., cytochrome P450, peroxidase). Despite the differences in

the chemistry they support, all these proteins share the common iron protoporphyrin IX (heme) as their prosthetic group. The functional variability of these proteins can be explained in terms of how the protein matrix interacts with the heme group and its potential substrates.

It has been of immense interest to understand the way in which protein structure influences heme reactivity towards stabilizing one particular oxidation state of iron over the other, or reactivity towards ligands. Redox potential is a thermodynamic property of heme proteins which can tell us about the structural features present in heme-binding cavities. The presence of different axial ligands for different heme proteins plays a crucial role in modifying the heme environment around the iron atom and hence has a direct impact on the reduction potential for the proteins (*14-22*). Depending on the number and nature of axial ligands around the iron in the heme prosthetic group, the coordination environment of heme could be modulated. For example, the heme iron in electron transfer protein (cytochrome *b5*), is tightly coordinated with histidine residues at both axial sites and does not bind small molecule ligands like dioxygen or peroxide. Whereas for oxygen storage or transport protein (myoglobin), central iron atom is only linked to the proximal axial ligand and can accept molecular oxygen or other exogenous ligands in the vacant distal site.

On the contrary, the newly discovered hxHbs have the similar coordination environment as that of cytochrome *b5*, but surprisingly, the exogenous ligands can compete with the distal axial His for binding. Due to so much diversity in coordination characteristics of the heme moiety, the effects of axial ligand mutations have been studied for a large number of heme proteins such as myoglobin, cytochrome *b5* (cyt *b5*), and

cytochrome *c* (cyt *c*) for decades. For example, Raphael and Gray reported (*15, 16*) that substitution of the axial ligand Met-80 of cytochrome *c* by Cys or His could decrease the reduction potential of the mutants to a great extent (cyt *c*-Cys80: -390mV and cyt *c*-His80: 41mV) compared to the native cyt *c* potential value (262mV). The reduction potential of cyt *c*-Cys80 is found to be close to the reduction potential of native cyt P450; similarly, cyt *c*-His80 has its reduction potential comparable to that of cyt *b5* (Table 1.1). This could be rationalized by the fact that above are the examples in which Fe has similar coordination environment in respective pairs.

Likewise, Rordriguez & co-workers showed (*17*) that replacement of one of the heme axial ligands, His63, in outer mitochondrial membrane cytochrome *b5* (OM cyt *b5*) by Met could give rise to a much higher reduction potential value (+110mV) just like pentacoordinate Mb (+50 mV) compared to the wild type OM cyt *b5* (-102 mV). Addition of exogenous imidazole to the variant protein could retrieve the hexacoordination character just like the wild type protein and the potential almost returns to the wild type potential value (-90 mV). Adachi & co-workers (*18*) claimed that the mutation of the axial ligand of human Mb with Cys resulted in extremely low reduction potential (H93C Mb: -230 mV) compared to the wild type protein (+50mV) which becomes close to the cyt P450 potential since the coordination feature of the mutant protein resembles that of the cyt P450 (Fe^{3+} species linked to the proximal thiolate).

Table 1.1 Redox potentials (Fe^{3+}/Fe^{2+} couple) of various heme proteins.

Protein	Redox Potential (mV)	Reference
SwMb[a](wt)[b]	59	(*23*)
H64L[c]	84	
H64G[d]	65	
H64V[e]	76	
Human Mb(wt)	50	(*18*)
H93C	-230	
H93Y	-190	
SwMb(wt)	58.8	(*24*)
V68E	-136.8	
V68D	-132.1	
V68N	-23.8	
Pig and Human Mb(wt)	54	(*25*)
H64V/V68H	-128	
Lba[f]	21	(*26*)
L88D	-14	
Cytochrome *c*	262	(*27*)
Cyt *c*-His80	41	(*15*)
Cyt *c*-Cys80	-390	(*16*)
Horse radish peroxidase	-250	(*28*)
Cytochrome P-450	-360 to -170	(*29*)
Cytochrome *b5*	5	(*30*)
OM cyt *b5*[g]	-102	(*17*)
H63M	110	
H63M+Imidazole	-92	
Mouse Ngb[h]	-129	(*31*)
*Syn*Hb	-150	(*32*)
Human Cgb(wt)[i]	20	(*33*)
H81A, H113A	-80 to -90	

[a]Sperm whale myoglobin; [b]Wild-type protein; [c]Leucine, [d]Glycine, [e]Valine mutants of distal histidine (His64) residue of sperm whale myoglobin and the other such representations in other rows correspond mutants of the respective wild type proteins; [f]Pentacoordinate hemoglobin found in leguminous plants, Leghemoglobin; [g]Outer mitochondrial Cytochrome *b5*; [h] Hemoglobin found in nervous cell, Neuroglobin; [i]Recombinant Cytoglobin

In addition to the coordination features, the electrostatic environment in the heme cavity can affect the redox behavior of these proteins. Van Dyke & co-workers (*23*) showed that a single point mutation of distal His64 of sperm-whale myoglobin with non-

polar residues (Val, Leu, Met, Gly, and Phe) can lead to much pronounced redox behavior than the wild type protein (+59mV) due to lower reorganization energy requirement in absence of extended H-bonding network in the distal pocket. Varadarajan & co-workers demonstrated (*24*) that by introducing some polar residues Glu, Asp, Asn in place of Val68 in the distal pocket of human Mb can lower the reduction potential value up to -200 mV for Glu and Asp mutants and -80mV for Asn mutant with respect to the wild type potential due to the higher stabilization of the Fe^{3+} oxidation state by electron rich centre in the vicinity of Fe. Thus, from the above studies it may be concluded that the inner-sphere-co-ordination effects and electrostatics at the metal-protein interface have been found to control the reduction potential in metalloredox proteins. All the above mentioned redox potential values are taken from the existing literature and Table1.1 contains a list of those reported potential values.

Distal Histidine coordination of hxHbs studied by electrochemistry and equilibrium binding experiments

The redox potential of (Fe^{3+}/Fe^{2+}) redox couple in heme proteins can reveal bonding, electrostatic interactions at the redox center and conformational shifts associated with a change in oxidation state (*34*). All hxHbs (measured so far) have lower reduction potentials than pentacoordinate Hbs, and the degree to which this value is affected is related to the differential strength of distal histidine (His^{hx}) coordination in the ferric *versus* the ferrous oxidation state. We wanted to raise the question in our study whether this differential His^{hx} coordination of hxHbs is directly related to their potential function and whether this effect is regulated in similar or different ways for all the members of

hexacoordinate family. Another related question follows thereafter: why is hexacoordination so important for these proteins. If hxHbs were simply electron transfer proteins (like cytochrome *b5*), or simply ligand transporters (like the pentacoordinate Hbs), there would be no need for displaceable hexacoordination. Thus it is likely that reversible hexacoordination is a component of hxHb functionality, and an investigation of the contribution of the protein matrix in this phenomenon will provide insight into their physiological roles.

The experiments in chapter 3 focus on the electrochemical and equilibrium ligand binding studies testing the role of the protein matrix on His^{hx} coordination in a set of hxHbs representing animals, plants, and bacteria that includes human Ngb and Cgb, rice nsHb (RHb1), and *Synechocystis* cyanoglobin (*Syn*Hb). The impact of the protein matrix on coordination is achieved by comparing data from two "equivalent" ligand states, one where the distal histidine ligand is covalently linked with the protein matrix, and the other with the ligand independent of the protein matrix. This is done with a set of experiments measuring the reduction potentials of each wild type hxHb and its corresponding mutant protein where the reversibly bound histidine (the distal His) has been replaced with a non-coordinating side chain. These reduction potentials, coupled with studies of the mutant proteins saturated with exogenous imidazole, enable us to assess the effects of the protein matrices on distal histidine coordination. The binding of exogenous imidazole to the mutant proteins has also been investigated by equilibrium binding experiments for both oxidation states of iron to complement the electrochemical measurements. It was evident from the experiments that significant variation exists among the hxHbs, demonstrating flexibility in the globin moiety's ability to regulate reversible coordination (*35*).

Carbon monoxide (CO) binding studies of hxHbs by electrochemistry

Pentacoordinate hemoglobins (mammalian Hb and myoglobin) generally bind small molecule ligands like oxygen (O_2), carbon monoxide (CO) in the ferrous state; cyanide (CN^-), azide (N_3^-) in the ferric state. Some physiologically relevant ligand like nitric oxide (NO) can bind these proteins in both oxidation states. Though CO is not so obviously physiologically important like O_2 or NO, plenty of ligand binding studies with CO have been performed with these proteins for past several years. One of the reasons for that is CO has often been given the role of understudy to the reactive dioxygen molecule in the analysis of ligand binding. Another important aspect of CO ligation is the search for the structural discrimination between O_2 and CO.

Hexacoordinate hemoglobins have an extraordinary feature of binding external ligands by replacing the reversibly bound distal histidine. While hxHbs can bind oxygen and other exogenous ligands, the kinetic and equilibrium behavior of the reactions are much more complex than the simple bimolecular reactions observed with pentacoordinate Hbs due to competition of the reversible intramolecular coordination of the binding site. Since physiological role for hxHbs has not been assigned with certainty yet, one of the potential roles could be traditional ligand binding. So a thorough investigation of ligand binding studies for hxHbs is mandatory to reveal their true physiological role in exclusion of others. The usual kinetic methods (flash photolysis, rapid mixing experiments) employed for the ligand binding studies of pentacoordinate proteins are of limited use for hxHbs due to multi-phasic time courses for O_2 and CO binding which can not predict any simple reaction model of ligand binding for these proteins (*1, 4, 31, 36, 37*). Thus there is a

need to develop other techniques which can complement the measurements obtained from the kinetic study.

The three most commonly used methods for determining the equilibrium constants of the axial ligation of heme proteins are UV-visible spectroscopy, NMR spectroscopy and electrochemical techniques. Electrochemical methods are preferred from an experimental point of view because; in one set of experiments the equilibrium constants of both Fe (III) and Fe (II) can be evaluated (*34*). Furthermore, the reduction potentials for the redox couple in presence and absence of axial ligands can be studied from the same set of data. This is also a direct and straightforward method of calculating the affinity constants just from a single experiment whereas the conventional techniques (stopped flow and flash photolysis methods) used for Hbs need more than one different set of experimental data to extract the values for affinity constants.

The experiments in chapter 4 reveal the equilibrium binding study of hxHbs with CO monitored by electrochemical methods. This study is achieved by monitoring the reduction potential of a set of hxHbs from different species like human Ngb and Cgb, plant rice nsHb (RHb1), and bacterial *Synechocystis* cyanoglobin (*Syn*Hb) with variable concentrations of CO. The equilibrium constant for the CO binding can be determined by monitoring the change in reduction potentials for the wild type variety without CO and the potential for the same protein with different concentrations of CO. The CO binding studies of His^{hx} mutants of hxHbs have been attempted to be performed in the same way as that of the wild type proteins but the study could not be proceeded further due to some unusual event of reduction of ferric mutant proteins in presence of CO. This reduction, accomplished under a CO atmosphere in the absence of other added reductants, has been

referred to as "autoreduction" which was also observed (albeit much more slowly) with cytochrome *c* oxidase in the ferric state and also for oxidized forms of heme and oxygen binding proteins like hemoglobin and myoglobin (*38*) . The reductive reaction for the ferric mutant proteins of hxHbs was monitored by their spectral changes observed in presence of CO.

CHAPTER 2: MATERIALS AND METHODS

Protein Production

The generation of the expression plasmids for the wild type hxHbs and their His^{hx} Leu and Ala substitutions ($His^{hx}L$ and $His^{hx}A$) in addition to protein expression and purification has been described earlier (*4*). In brief, the cDNAs coding for each wild type protein were inserted into the pET28a vector (Novagen) and the resulting plasmids were used with Stratagene's QuickChange site-directed mutagenesis kit to generate mutant cDNAs. *Escherichia. Coli* (DE3) harboring pET28-hxHbs plasmids were grown in TB at 37°C overnight, with protein over-expression achieved by autoinduction. Following cell lysis, $NonHis_6$-tagged proteins (RiceHb, *Syn*Hb and their His^{hx} mutants) were purified by using a four-stage protocol including ammonium sulfate fractionation, hydrophobic (Phenyl Sepharose), anion-exchange (DEAE Sepharose) and size exclusion (Sephacryl S-200) chromatography. For His_6-tagged proteins (Cgb, Ngb and their His^{hx} mutants), purification was accomplished with an affinity column (nickel-nitrilotriacetic acid) followed by size-exclusion chromatography. Horse heart myoglobin was obtained commercially from Sigma®. Prior to electrochemical titration and imidazole binding, all proteins were oxidized with an excess of potassium ferricyanide, which was removed by passage through a Sephadex G-25 column equilibrated in 0.1 M potassium phosphate buffer (pH 7.0). All proteins were stored at -80°C.

Spectroelectrochemistry (SEC)

Potentiometric titrations were performed using the method described by Altuve and co-workers (*39*), with an Ocean-Optics UV-VIS spectrophotometer (USB2000) and Oakton pH-mV meter (pH 1100 Series). A saturated calomel electrode (SCE) was used as a reference in combination with a platinum working electrode. Reduction potentials (E_{obs}) and mid-point potentials (E_{mid}) are reported with reference to a standard hydrogen electrode (SHE). A custom-made electrochemical cell was employed for all the measurements (Figure 2.1). It was originally made up of a quartz cuvette joined with the upper glass extension of the cell by special quartz to glass gradient seal. The upper portion of the cell has three openings, among them, the top one was used for inserting the electrodes into the cell solution through an air-tight rubber stopper. The side arm openings of the cell were sealed with open-top plastic caps fitted with air-tight teflon septa. One arm was used for the gas inlet and the other for the gas outlet and for addition of mediators, proteins and the reductant (dithionite solution) via an air-tight glass syringe attached with a flexible long needle. All the above features of the cell were adopted to ensure an anaerobic condition (with argon) during the experiment. Argon was passed through an oxygen scavenging solution to remove the traces of oxygen impurity before purging into the cell. The cell was kept in a temperature-controlled cuvette holder placed on the top of a magnetic stirrer. Titrations of ~20 μM Hb were carried out at 25 °C in argon-saturated 0.1M potassium phosphate buffer, pH 7.0 with a set a redox mediators buffering the entire potential range of the studied proteins. Ferric proteins were titrated stepwise with a sodium dithionite solution (40 mM) previously sparged with argon. Reactions were monitored by recording the absorbance spectra of deoxy ferrous proteins in the visible region (500-700

nm), and the corresponding cell potential (E_{obs}) was noted for each addition of dithionite solution after attainment of equilibrium.

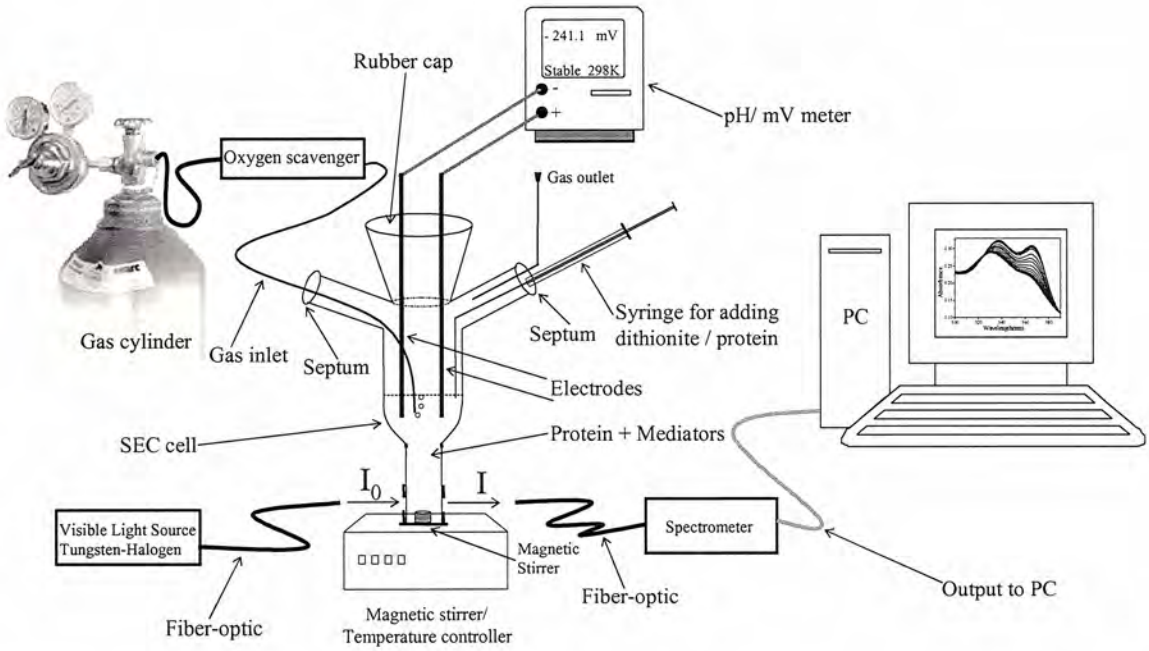

Figure 2.1 The spectroelectrochemistry set-up for potentiometric titration of heme proteins.

The group of redox mediators was used to buffer the potential range from +160 to -440 mV. Their standard reduction potential vs. SHE are: 1,2-naphthoquinone (E_{mid} = +157 mV), toluylene blue (E_{mid} = +115 mV), duroquinone (E_{mid} = +5 mV), hexaammineruthenium (III) chloride (E_{mid} = +50 mV), pentaminechlororuthenium (III) chloride (E_{mid} = -40 mV), 5,8-dihydroxy-1,4-naphthoquinone (E_{mid} = -50 mV), 2,5-dihydroxy-1-4 benzoquinone (E_{mid} = -60 mV), 2-hydroxy-1,4-naphthoquinone (E_{mid} = -137mV), anthraquinone-1,5-disulfonic acid (E_{mid} = -175 mV), 9,10-anthraquinone-2,6-disulfonic acid (E_{mid} = -184 mV), and methyl viologen (E_{mid} = -440 mV).

Extraction of mid-point potential from the absorbance of deoxy ferrous species and corresponding observed reduction potentials

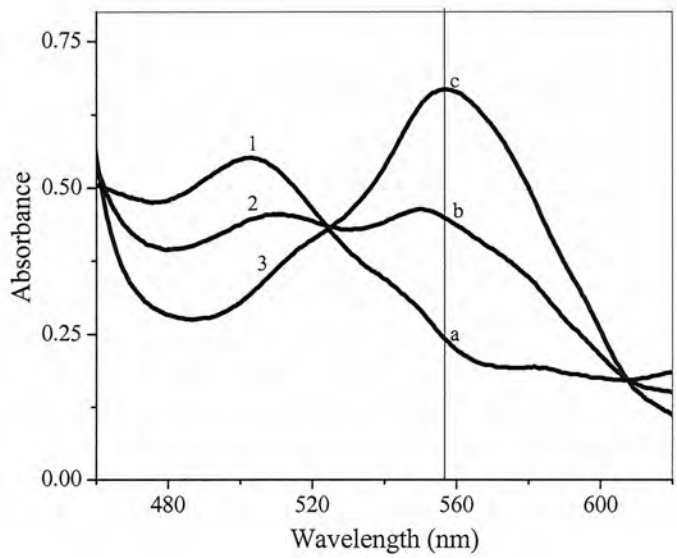

Figure 2.2 Typical electrochemical titration experiment showing the absorbance spectra of fully oxidized, intermediate reduced and fully reduced species.

The above set of spectra is a schematic representation of the electrochemical titration experiment where '1', '2', '3' correspond the absorbance spectra of fully oxidized (ferric) form, intermediate reduced form and fully reduced (ferrous) form of the protein. Their absorbances are a, b, c at the wavelength maxima of the deoxy ferrous protein for the above three cases respectively. The total change in absorbance at that wavelength is given by, $\Delta Abs_{tot} = a\text{-}c$. The change in absorbance for the intermediate reduced species is, $\Delta Abs_{int} = a\text{-}b$. So, fraction of reduced protein (F_{red}) can be determined by the following ratio

$$F_{red} = \frac{\Delta Abs_{\text{int}}}{\Delta Abs_{tot}} = \frac{a-b}{a-c} \qquad \text{Equation 2.1}$$

The Nernst equation for oxidation-reduction reaction is as follows:

$$E_{obs} = E^0 + \frac{RT}{nF} \ln \frac{[Ox]}{[\mathrm{Re}d]} \qquad \text{Equation 2.2}$$

Here, E_{obs} is the measured cell potential; E^0 is the cell potential for components in their standard state; T is the absolute temperature; R is the gas constant; [Ox] is the concentration of the oxidizing species and [Red] is the concentration of the reducing species.

Equation 2.2 can be re-written as:

$$E_{obs} = E^0 + \frac{RT}{nF} \ln \frac{F_{ox}}{F_{red}} \qquad \text{Equation 2.3}$$

Where, F_{ox} is the fraction of oxidized species and F_{red} is the fraction of reduced species.

When the reaction is half-complete (i.e.; $F_{ox} = F_{red}$) then the corresponding equilibrium potential is known as the mid-point potential (E_{mid}) of the protein (i.e.; $E^0=E_{obs}=E_{mid}$).

Equation 2.3 becomes:

$$E_{obs} = E_{mid} + \frac{RT}{nF} \ln \frac{F_{ox}}{F_{red}} \qquad \text{Equation 2.4}$$

Now by rearranging equation 2.4 and substituting the value of F_{ox} in terms of F_{red} from the expression, $F_{ox}+F_{red}=1$,

$$\frac{1-F_{red}}{F_{red}} = e^{\left(\frac{nF(E_{obs}-E_{mid})}{RT}\right)} \qquad \text{Equation 2.5}$$

After the mathematical simplification, F_{red} can be expressed in terms of the potential as follows (*40*):

$$F_{reduced} = \frac{e^{-\left(\frac{nF(E_{obs}-E_{mid})}{RT}\right)}}{1+e^{-\left(\frac{nF(E_{obs}-E_{mid})}{RT}\right)}}$$ Equation 2.6

Midpoint potentials were extracted from fraction of protein reduced (Equation 2.1) and the observed potential corresponding to each addition of dithionite by fitting to the above Equation 2.6.

$F_{reduced}$ is the normalized change in absorbance at ~560 nm, E_{obs} is the observed reduction potential, and E_{mid} is the midpoint potential obtained by fitting the experimental data to Equation 2.6. Midpoint reduction potentials for imidazole-saturated His^{hx} mutant proteins were measured as described above, except that the reaction buffers contained concentrations of imidazole sufficient to saturate both the ferric and ferrous forms of each protein. The necessary imidazole concentrations for each experiment were measured empirically (described below) as: 200 mM (RHb1:His^{hx}L), 300 mM (Cgb:His^{hx}L), 300 mM (Ngb:His^{hx}L), and 1 mM (Syn:His^{hx}L).

Equilibrium imidazole binding to His^{hx} mutant proteins

Imidazole affinity constants for each His^{hx} mutant protein were measured by spectrophotometric titrations with a Cary50-UV-Vis Spectrophotometer. 1 cm cuvettes with ~ 10 μM solutions of each His^{hx} mutant protein were prepared in 0.1 M potassium phosphate buffer, pH 7.0. A solution of imidazole in the same buffer was used to titrate the Fe^{3+} and Fe^{2+} forms of each mutant protein at room temperature. Ferric protein titrations were carried out in air, and ferrous protein titrations were carried out in a sealed

cuvette with nitrogen-equilibriated buffer containing 100 μM sodium dithionite. Equilibrium association constants for imidazole ($K_{3,Im}$ and $K_{2,Im}$ as in Scheme 3.1 of chapter 3) for the mutant proteins were calculated by fitting the titration data to Equation 2.7, where F_B is the fraction of protein bound to imidazole at each imidazole concentration [Im] (*41, 42*).

$$F_B = \frac{K_{Im}[Im]}{1 + K_{Im}[Im]} \qquad \text{Equation 2.7}$$

CO binding studies of hxHbs by electrochemical methods

Reduction potentials of hxHbs have been measured in absence and presence of different concentrations of CO. The CO binding studies were done using the same electrochemistry set-up described above. Instead of using the constant flow of argon prior and during the experiment, these experiments were performed under a constant CO atmosphere. Solubility of CO at 25°C and under 1 atm pressure is known to be 1000uM. The experimental CO concentrations were 5, 10, 50 and100 μM. For 100 and 10μM CO concentration experiments, a gas cylinder of 10% CO and 1% CO balanced with nitrogen was used respectively. For the other two working CO concentrations (50 and 5 μM), desired concentrations of CO were maintained by mixing 10% CO or 1% CO and nitrogen in equal ratio by a regulating flow tube before passing to the cell. The idea is that the amount of CO that would be present in solution depends on its partial pressure in the gas mixture. So, at equal partial pressure of CO and N_2, the concentration of CO will be reduced to half with respect to 10% or 1% CO concentration values. Reduction potentials for CO experiments were extracted by using the same equation 2.6 in absence and presence

of CO. From the difference in mid-point potentials the affinity constants of hxHbs for CO have been calculated.

CHAPTER3: HISTIDINE LIGATION IN HEXACOORDINATE HEMOGLOBINS

Introduction

Hemoglobins (Hbs) are proteins that bind iron protoporphyrin IX (heme *b*) by using a conserved alpha-helical globin fold. The iron atom in the heme group typically exists in either the ferrous (Fe^{2+}) or ferric (Fe^{3+}) oxidation state, with both capable of octahedral coordination geometry. Heme pyrrole nitrogens fill the four equatorial binding sites, and one of the two axial sites (the proximal) is occupied by a histidine side chain that is invariant in the Hb super-family. The remaining (distal) axial site is where binding of small ligands takes place, such as O_2 and CO in the ferrous state, or CN^- and N_3^- in the ferric state. Some physiologically important ligands like NO can bind Hbs in both oxidation states.

In the absence of exogenous ligands, the distal binding site is vacant in many Hbs (such as mammalian Hb and myoglobin) and they are thus referred to as "pentacoordinate" Hbs. However, other globins have been found in plants, animals, and bacteria that are not pentacoordinate in the absence of exogenous ligands. In these proteins the distal axial coordination site is occupied by another histidine side chain (His^{hx}) in both oxidation states, giving rise to their designation as "hexacoordinate Hbs" (hxHbs) (*1-3*). Examples of hxHbs include neuroglobin (Ngb) and cytoglobin (Cgb) in animals, the nonsymbiotic Hbs (nsHbs) found in plants, and some of the truncated Hbs found in bacteria. Although the respiratory function is typically associated with the pentacoordinate Hbs, a physiological role for hxHbs has yet to be assigned with certainty (*7-11*). It has, however, been

demonstrated that intramolecular hexacoordination exerts significant influence on ligand binding and redox properties (*14-22*).

There are several attributes that hexacoordination could contribute to Hb function. It is a mechanism for regulating ligand affinity (*1, 3*), it facilitates reduction kinetics (*43*), and can promote a large change in protein conformation upon exogenous ligand binding (*44*). These features are a key reason for the diverse physiological roles postulated for hxHbs, which range from ligand sensing and transport to NO scavenging and signal transduction (*12*). A central question about hxHbs is the role of the protein matrix (that is, the globin moiety of the Hb) on hexacoordination behavior; does the protein promote or hinder intramolecular histidine coordination?

This question is crucial to our understanding of the functionality of hxHbs. Both cytochrome *b5* and the hxHbs use *bis*-histidyl coordination of the heme prosthetic group, yet they are structurally quite different (Figure 3.1A). And while cytochrome *b5* and hxHbs share the same heme ligation state, their protein matrices result in a marked difference in intramolecular hexacoordination behavior; the globin facilitates reversible histidine binding (and thus enables exogenous ligand binding) while the cytochrome does not. If hxHbs were electron transfer proteins (like cytochrome *b5*), or ligand transporters (like the pentacoordinate Hbs), there would be no need for displaceable hexacoordination. Thus it is likely that reversible hexacoordination is a component of hxHb functionality, and an investigation of the contribution of the protein matrix in this phenomenon will provide insight into their physiological roles.

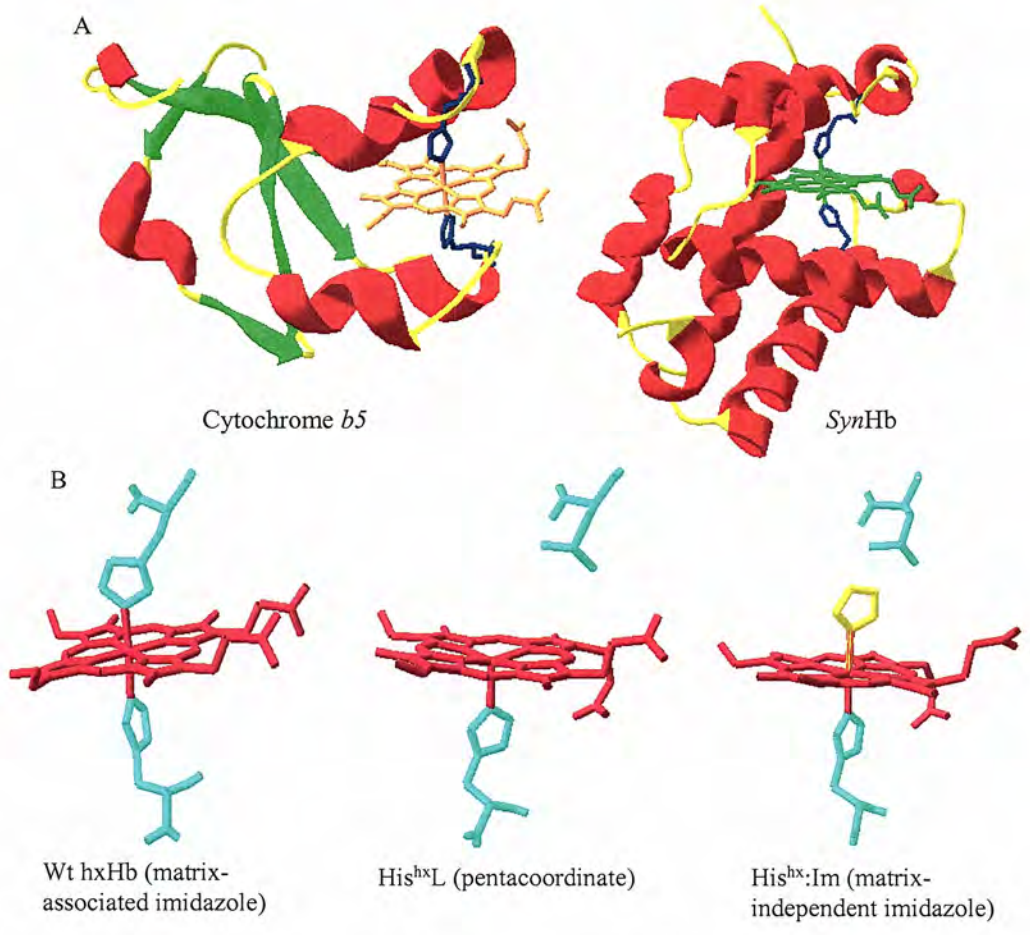

Figure 3.1 Crystal structures of cytochrome *b5* (Protein Data Bank code 1CYO) and *Syn*Hb (1RTX) illustrating the *bis*-histidyl heme cofactor associated with different protein matrix structures **(A)**. Structural models comparing the three forms of hxHbs that collectively enable isolation of hexacoordination from protein matrix effects in this work **(B)**.

Electrochemistry is a powerful tool for studying heme proteins. Many aspects of the protein can be revealed by monitoring redox potential, such as bonding, electrostatic interactions at the redox center and conformational shifts associated with a change in oxidation state (*45*). All hxHbs (measured so far) have lower reduction potentials (*31, 32*) than pentacoordinate Hbs (*46, 47*), and the degree to which this value is affected is related to the differential strength of His^{hx} coordination in the ferric *versus* the ferrous oxidation

state. Thus electrochemistry provides a corroborative complement to equilibrium binding in measuring whether the protein has evolved to augment the innate chemical tendency toward hexacoordination, or inhibit tight coordination to facilitate exogenous ligand binding.

Here we present electrochemical and equilibrium ligand binding studies testing the role of the protein matrix on His^{hx} coordination in a set of hxHbs representing animals, plants, and bacteria that includes human Ngb and Cgb, rice nsHb (RHb1), and *Synechocystis* cyanoglobin (*Syn*Hb). This work assesses the impact of the protein matrix by comparing data from two "equivalent" ligand states, one where the ligand is associated with the protein matrix, and the other with the ligand independent of the protein matrix (Fig. 3.1B). Our results suggest that only the plant hxHbs significantly modulate hexacoordination through the protein matrix.

Results

General methodology

The goal of these experiments was to measure the effects of the protein matrix on hexacoordination in the ferrous and ferric oxidation states of several hxHbs. Binding of the His^{hx} side chain in the wild-type proteins is thermodynamically linked to reduction potentials, as is exogenous ligand binding to the His^{hx} mutant proteins. Thus our results are derived from the measurement of four fundamental values, which are illustrated in Scheme 3.1.

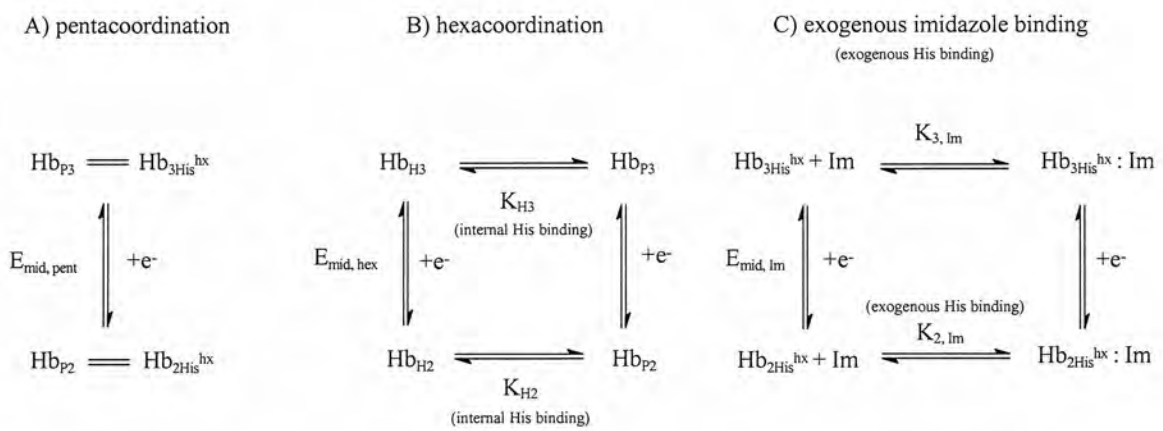

Scheme 3.1 Pertinent reactions associated with exogenous imidazole binding and reduction potentials in hxHbs and their His^{hx} mutant proteins. Hb_P is the pentacoordinate Hb in either the ferrous (2+) or ferric (3+) oxidation state. Hb_{His}^{hx} is the mutant hxHb in which the hexacoordinating His side chain has been replaced by an amino acid incapable of coordination. Hb_H is the hexacoordinate Hb, and "Im" is exogenous imidazole.

These values are: 1) The midpoint reduction potential of the "pentacoordinate" form of each hxHb ($E_{mid,pent}$), as measured by using its surrogate His^{hx} mutant protein (Scheme 3.1 A). 2) The relative values of K_{H3} and K_{H2} (Scheme 3.1 B), as measured by comparing $E_{mid,pent}$ to the midpoint reduction potential of the wild type hxHb ($E_{mid,hex}$). 3) The affinity of the His^{hx} mutant proteins for free imidazole in the ferrous ($K_{2,Im}$) and the ferric ($K_{3,Im}$) oxidation states (Scheme 3.1 C), as measured directly by equilibrium titration. 4) Measurement of $E_{mid,Im}$ provides an independent measurement of $K_{2,Im}/K_{3,Im}$ for comparison to that obtained by equilibrium titration. By comparing K_{H3}/K_{H2} (the ratio of His^{hx} affinity in different oxidation states for the wild type protein) to $K_{3,Im}/K_{2,Im}$ (the ratio for the His^{hx} mutant protein in which the imidazole is not bonded to the protein matrix) the effects of the protein matrix on imidazole coordination can be measured.

Thermodynamic relationships between His^{hx} hexacoordination, exogenous imidazole binding, and reduction potentials

The effect of intramolecular coordination on the midpoint potential of a Hb is described by the following equation (derived from the reactions in "B" of Scheme 3.1) (*40*).

$$F_{reduced} = \frac{e^{-\left(\frac{nF\left(E_{obs}-E_{mid,pent}\right)}{RT}\right)}}{\left(\frac{1+K_{H3}}{1+K_{H2}}\right)+e^{-\left(\frac{nF\left(E_{obs}-E_{mid,pent}\right)}{RT}\right)}} \qquad \text{Equation 3.1}$$

When $F_{reduced} = 0.5$, $E_{obs} = E_{mid,hex}$. This results in a simplified relationship (Equation 3.2) between the hexacoordination affinity constants in each oxidation state and the midpoint reduction potentials of the penta- and hexacoordinate forms of the protein.

$$\left(\frac{1+K_{H3}}{1+K_{H2}}\right) = e^{-\left(\frac{nF\left(E_{mid,hex}-E_{mid,pent}\right)}{RT}\right)} \qquad \text{Equation 3.2}$$

If the absolute values of K_{H2} and K_{H3} are large, the "1+" on the left is insignificant and the difference in midpoint potentials is directly related to the ratio of affinity constants. As K_{H2} and K_{H3} approach zero, or if they are equal, there will be no difference in midpoint potential between the penta- and hexacoordinate forms of the protein.

The effects of exogenous imidazole binding are slightly different, and described by the following equation (derived from the reactions in "C" of scheme 3.1).

$$F_{reduced} = \frac{e^{-\left(\frac{nF\left(E_{obs}-E_{mid,pent}\right)}{RT}\right)}}{\left(\frac{1+K_{3,Im}[Im]}{1+K_{2,Im}[Im]}\right)+e^{-\left(\frac{nF\left(E_{obs}-E_{mid,pent}\right)}{RT}\right)}} \qquad \text{Equation 3.3}$$

The same simplification resulting in Equation 3.2 can be made here:

$$\left(\frac{1+K_{3,\mathrm{Im}}[\mathrm{Im}]}{1+K_{2,\mathrm{Im}}[\mathrm{Im}]}\right)=e^{-\left(\frac{nF\left(E_{mid,\,\mathrm{Im}}-E_{mid,\,pent}\right)}{RT}\right)} \qquad \text{Equation 3.4}$$

However, in this case [Im] can be raised experimentally so that Equation 3.4 reduces to Equation 3.5.

$$\left(\frac{K_{3,\mathrm{Im}}}{K_{2,\mathrm{Im}}}\right)=e^{-\left(\frac{nF\left(E_{mid,\,\mathrm{Im}(sat)}-E_{mid,\,pent}\right)}{RT}\right)} \qquad \text{Equation 3.5}$$

This shows that the difference in midpoint potentials between the Hb in the absence of exogenous imidazole ($E_{mid,pent}$), and the Hb when saturated in both oxidation states ($E_{mid,Im(sat)}$) is directly related to the ratio of affinity constants in each oxidation state.

RHb1 and Cgb

The spectral changes associated with potentiometric titration of RHb1 and RHb1:His^{hx}L are shown in Figures 3.2 A and B. Plots of $F_{reduced}$ *versus* E (observed cell potential) are shown in Figure 3.2 F. Fits of these data to Equation 2.6 yield a midpoint reduction potential of -143 mV for wild-type RHb1, and -30 mV for RHb1:His^{hx}L. Imidazole titrations of RHb1:His^{hx}L in the ferric (Figure 3.2C) and ferrous (Figure 3.2D) oxidation states provide association equilibrium constants equal to 72 ($K_{3,Im}$) and 0.09 ($K_{2,Im}$) mM^{-1}, respectively. Figure 3.2E shows the absorbance spectra associated with potentiometric titration of RHb1:His^{hx}L in the presence of 200 mM imidazole. A plot of $F_{reduced}$ *versus* E (3.2 F) for these data generates a value of $E_{mid,Im(sat)}$ = -201 mV.

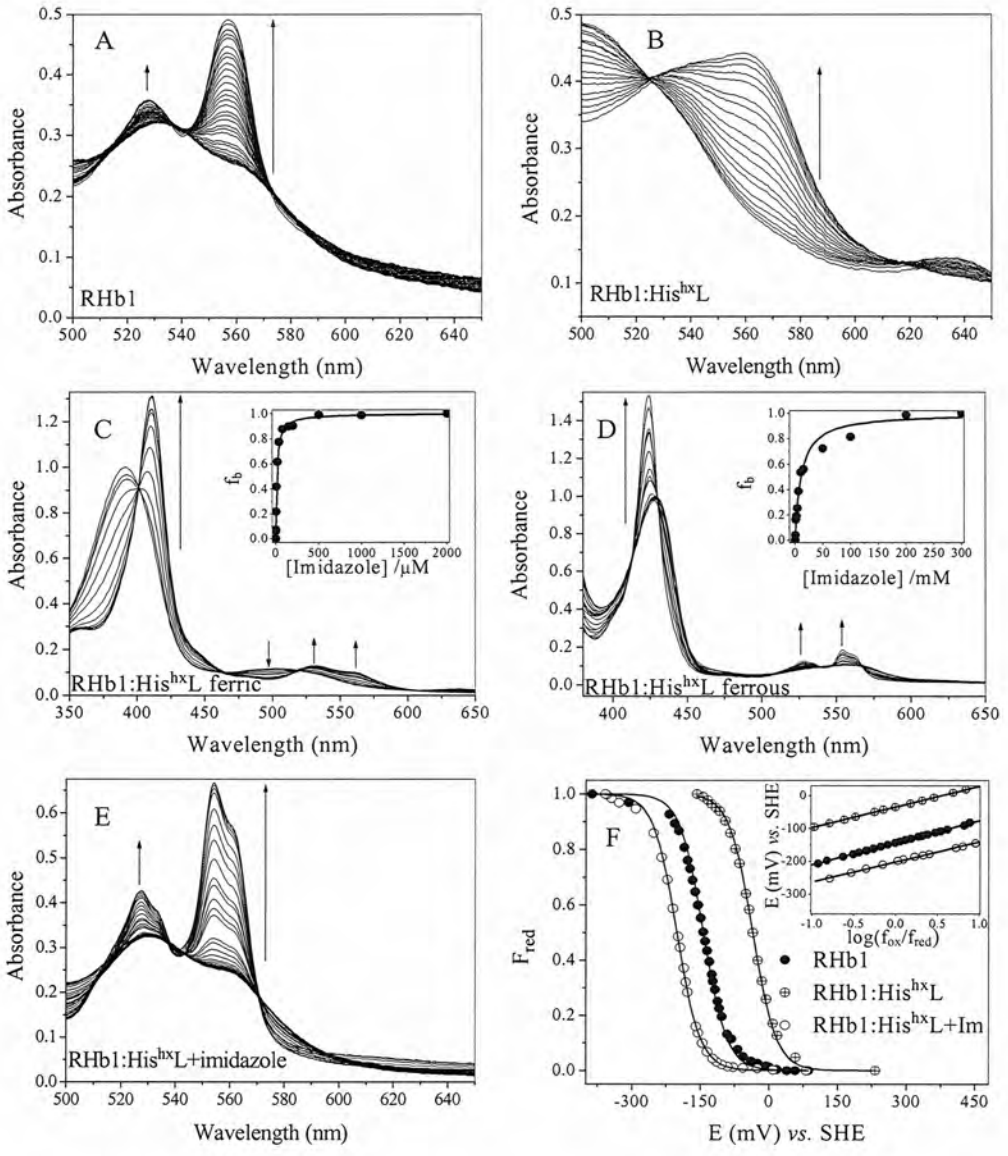

Figure 3.2 Reactions with RHb1. Spectroelectrochemical titrations of RHb1 (**A**) and RHb1:His^{hx}L (**B**). Equilibrium imidazole binding to RHb1:His^{hx}L in the ferric (**C**) and ferrous (**D**) oxidation states. The insets of C and D show the fitted curve for F_B as a function of imidazole concentration. (**E**) Spectroelectrochemical titrations of RHb1:His^{hx}L saturated with imidazole (200 mM). (**F**) The fraction of reduced protein (F_{red}) in each spectroelectrochemical titration as a function of E. Solid lines show the sigmoidal fit to Equation 2.6 with E_{mid} as the fitted parameter. The inset in F is Nernst plots of E *versus* $\log(F_{ox}/F_{red})$, with solid lines showing linear fits.

All these data are reported in Tables 3.1 and 3.2 along with some other information that can be interpreted as follows. "His^{hx} penta.?" reports whether the His^{hx} mutant protein for each hxHb is truly pentacoordinate (as measured by the absorption spectra in each oxidation state). This is an important consideration; if the His^{hx} mutant protein is not pentacoordinate, then its reduction potential cannot be used in Equation 3.4. $\Delta E_{wt\text{-}His}{}^{hx}{}_{L}$ in Table 3.1 is the difference between the wild-type and His^{hx} mutant reduction potentials, which can be used in Equation 3.2 to calculate $(1+K_{H3})/(1+K_{H2})$, the relative hexacoordination affinity constants in the ferric *versus* the ferrous oxidation state of the wild-type protein.

Table 3.1 Reduction midpoint potentials for wild type and $His^{hx}L$ hxHbs

protein	[a]$E_{mid,hex}$	His^{hx} penta.?	$E_{mid,His}{}^{hx}{}_{L}$	$\Delta E_{wt\text{-}His}{}^{hx}{}_{L}$	$(1+K_{H3})/(1+K_{H2})$
RHb1	-0.143	Yes	-0.03	-0.113	81
Cgb	-0.028	Yes	0.084	-0.112	78
Ngb	-0.115	No	-0.121	0.006	(325)[b]
*Syn*Hb	-0.195	No	-0.158	-0.037	(11)[b]
		No[c]	-0.153[c]	-0.042[c]	
Mb H64V/ V68H[d]	-0.128	Yes	0.076[e]	-0.204	2,800

[a]All potentials are in V vs. SHE and the measured potentials lie within an error limit of ±0.005V
[b]These values are calculated indirectly as described in the results section.
[c]These values are reported for His^{hx}A mutant of *Syn*Hb
[d]The value for H64V/V68H is taken from (*25*)
[e] The redox potential for H64V Mb (the pentacoordinate counterpart to H64V/V68H) is taken from (*23*)

Table 3.2 Imidazole binding to His^{hx} mutant proteins

protein	$K_{3,Im}$ (mM^{-1})	$K_{2,Im}$ (mM^{-1})	$K_{3,Im}/K_{2,Im}$	affinity ratio[f] (from titration)	$E_{mid,Im(sat)}$	affinity ratio[g] (from E.chem)
RHb1:His^{hx}L	72	0.09	800	9.8	-0.201	9.6
Cgb:His^{hx}L	26	0.17	150	2.0	-0.059	3.3
Ngb:His^{hx}L	52	0.16	325	nd	-0.115	1.0
*Syn*Hb:His^{hx}L	420	39	11	nd	-0.200	1.2
RHb1:His^{hx}A	190	0.2	950	-	-	-
*Syn*Hb:His^{hx}A	93	10	9.3	-	-	-

[f]calculated with Equation 3.6
[g]calculated with Equation 3.7

Table 3.2 reports the results of exogenous imidazole binding and its effects on the reduction potential of the His^{hx} mutant proteins. The imidazole affinity constant for each His^{hx} mutant protein is reported for the ferric and ferrous oxidation states along with the ratio of these values. A comparison of this ratio to $(1+K_{H3})/(1+K_{H2})$ for the wild type protein is described by Equation 3.6 as the "affinity ratio", and measures the degree to which the wild type protein facilitates or hinders His binding in the ferric *versus* the ferrous oxidation state.

$$\text{"affinity ratio"} = \frac{\left(\frac{K_{3,Im}}{K_{2,Im}}\right)}{\left(\frac{1+K_{H3}}{1+K_{H2}}\right)} \qquad \text{Equation 3.6}$$

An affinity ratio value >1 indicates that the wild type protein favors ferrous hexacoordination over ferric compared to free imidazole, whereas a value <1 indicates the opposite. Values near 1 assert that hexacoordination is not affected by the protein matrix.

In the case of RHb1 the $His^{hx}L$ mutant protein is pentacoordinate (as evident from the broad absorbance peaks in Figure 3.2B (*48*), which allows a meaningful calculation of $(1+K_{H3})/(1+K_{H2})$. This value for RHb1 is 81, indicating that hexacoordination is favored by this degree in the ferric state compared to the ferrous. However, the ratio of $K_{3,Im}/K_{2,Im}$ for RHb1:$His^{hx}L$ is 800, and the resulting affinity ratio of 10 means that the protein matrix is responsible for an order of magnitude decrease in the histidine side chain affinity of the ferric state compared to the ferrous.

The affinity constant for imidazole binding to a His^{hx} mutant protein provides a measure of the activity of the protein in the absence of hexacoordination. However, the nature of the substituted side chain is likely to have an effect on these absolute values, although it should not alter the ratio of affinities in each oxidation state. If affinity ratios were affected by the nature of the substituted side chain, then our results reported from this approach would represent a misinterpretation of the data. To validate these methods $K_{3,Im}$ and $K_{2,Im}$ were measured for the $His^{hx}A$ mutant protein of RHb1, and compared to the respective values for the $His^{hx}L$ substitution. The values of $K_{3,Im}$ and $K_{2,Im}$ for RHb1:$His^{hx}A$ are 190 mM^{-1} and 0.2 mM^{-1}, with a ratio of $K_{3,Im}/K_{2,Im}$ equal to 950 (Table 3.2). As predicted, the absolute values of each affinity constant are affected, but not the ratio of constants in different oxidation states.

An alternative method for determining the affinity ratio is described by Equation 3.7, which is obtained by dividing Equation 3.5 by Equation 3.2. It uses the reduction midpoint potential in the presence of saturating imidazole ($E_{mid,Im(sat)}$) in comparison to that of the wild type protein.

$$\text{"affinity ratio"} = \frac{\left(\frac{K_{3,\mathrm{Im}}}{K_{2,\mathrm{Im}}}\right)}{\left(\frac{1+K_{H3}}{1+K_{H2}}\right)} = e^{-\left(\frac{nF\left(E_{mid,\,\mathrm{Im}\,(sat)} - E_{mid,\,hex}\right)}{RT}\right)} \quad \text{Equation 3.7}$$

For RHb1 compared to RHb1:His^{hx}L:Im, this method yields an "affinity ratio" of 9.6, which is consistent with direct measurement of $K_{3,Im}$ and $K_{2,Im}$ (using Equation 3.6). This method for measuring the affinity ratio provides a means of corroborating values calculated using Equation 3.6. It also enables investigation of those hxHbs whose His^{hx} mutant proteins are not pentacoordinate and thus do not allow direct measurement of $E_{mid,pent}$, as is the case for Ngb and *Syn*Hb.

Potentiometric titration and imidazole binding data for Cgb are shown in Figure 3.3. As reported in Table 3.1, Cgb:His^{hx}L is pentacoordinate and has a significantly lower reduction midpoint potential than the wild-type protein. The resulting value of $(1+K_{H3})/(1+K_{H2})$ is similar to RHb1. However, $K_{3,Im}/K_{2,Im}$ is much lower for Cgb:His^{hx}L at 150 (Table 3.2). The resulting affinity ratio is only 2 and 3.3 as measured by the two different methods (Equations 3.6 and 3.7). This indicates that the protein matrix of Cgb disfavors ferric hexacoordination over ferrous by a factor of ~ 3 compared to free imidazole.

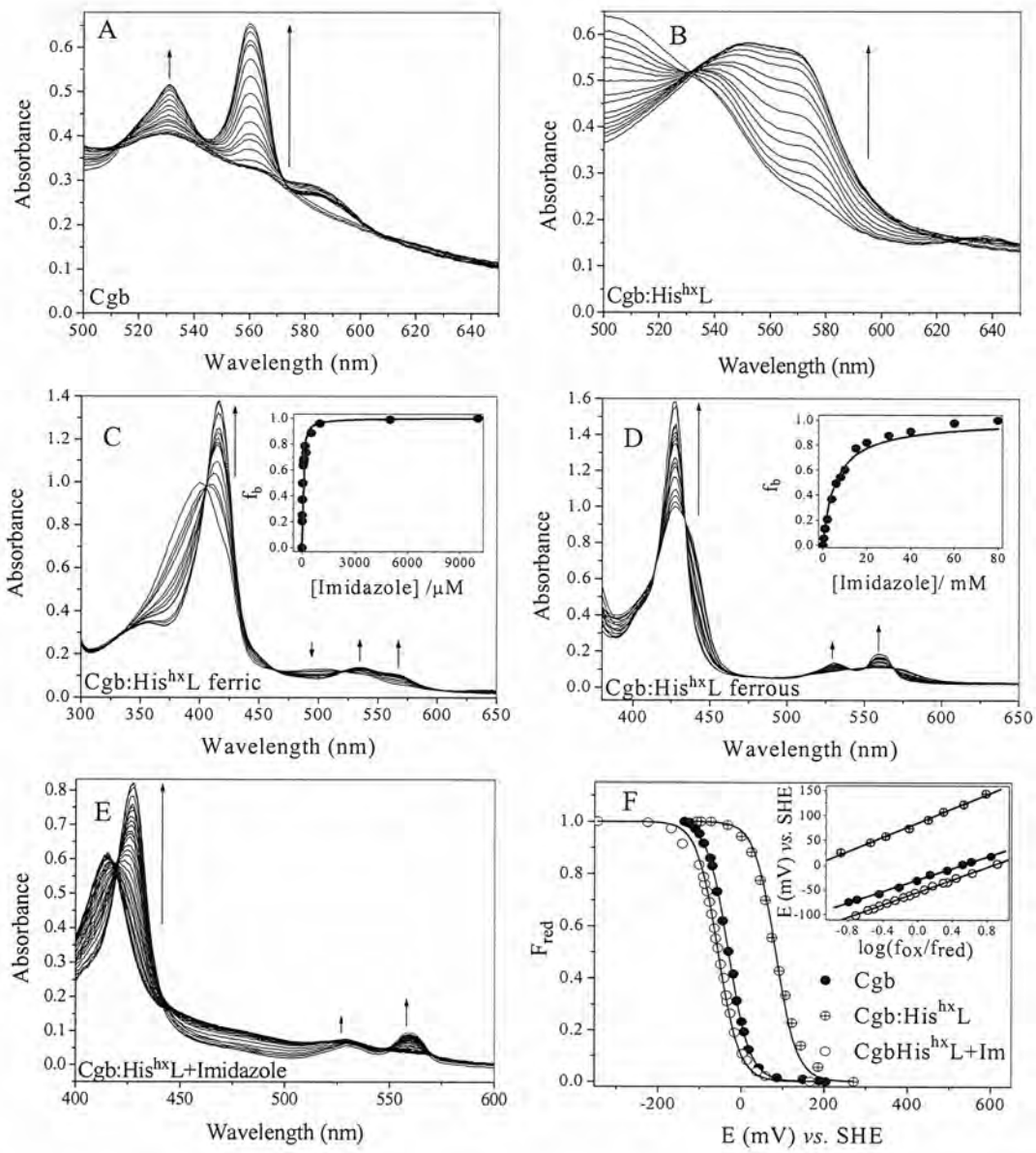

Figure 3.3 Reactions with Cgb. Spectroelectrochemical titrations of Cgb **(A)** and Cgb:His^{hx}L **(B).** Equilibrium imidazole binding to Cgb:His^{hx}L in the ferric **(C)** and ferrous **(D)** oxidation states. The insets of C and D show the fitted curve for F_B as a function of imidazole concentration. **(E)** Spectroelectrochemical titrations of Cgb:His^{hx}L saturated with imidazole (300 mM). **(F)** The fraction of reduced protein (F_{red}) in each spectroelectrochemical titration as a function of E. Solid lines show the sigmoidal fit to Equation 2.6 with E_{mid} as the fitted parameter. The inset in F is Nernst plots of E *versus* $\log(F_{ox}/F_{red})$, with solid lines showing linear fits.

Ngb and *Syn*Hb

Spectral changes associated with reduction of wild type *Syn*Hb and Ngb are shown in Figures 3.4A and 3.5A, and E_{mid} values for each were extracted by fitting the data in Figures 3.4F and 3.5F and are reported in Table 3.1. These values are similar to those reported previously (*31, 32*). However, the absorbance spectra of the $His^{hx}L$ mutant proteins of *Syn*Hb and Ngb reveal residual coordination in the absence of the His^{hx} side chain in both the ferrous and ferric oxidation states (Figures 3.4B and 3.5B). The source of coordination is not known, but is likely solvent (*5, 36, 37*). It is therefore of no surprise that reduction potentials of these mutant proteins do not reflect those expected for truly pentacoordinate Hbs (like the analogous proteins from RHb1 and Cgb). The lack of a shift to higher E_{mid} in the His^{hx} mutant proteins suggests that solvent binds more tightly to the ferric than the ferrous oxidation state (which is observed in many pentacoordinate Hbs (*49*)). The inability to measure $E_{mid,pent}$ precludes direct calculation of $(1+K_{H3})/(1+K_{H2})$ for these proteins, and calculation of the "affinity ratio" using Equation 3.6.

The ability of solvent to bind *Syn*Hb and Ngb $His^{hx}L$ mutant proteins is probably a consequence of relatively low association equilibrium constants offset by high solvent concentration, as free imidazole easily out-competes solvent binding in both cases. Therefore, $K_{3,Im}$ and $K_{2,Im}$ can be measured by equilibrium titration (Figures 3.4C and D and 3.5C and D, Table 3.2). Furthermore, a comparison of $E_{mid,Im(sat)}$ (Figures 3.4E and F and 3.5E and F) for the His^{hx} mutant proteins to $E_{mid,hex}$ in the wild type proteins allows calculation of the affinity ratios for *Syn*Hb and Ngb using Equation 3.7. The affinity ratio thus obtained for both of these proteins is near unity, indicating that the protein matrix in each has little effect on coordination of imidazole in the ferrous *versus* the ferric oxidation

states. These values are included in Table 3.1 along with the values of $(1+K_{H3})/(1+K_{H2})$ for the other hxHbs.

The effect of the nature of side chain substitution on the values of $K_{3,Im}$ and $K_{2,Im}$ was also measured for the $His^{hx}A$ mutant protein of *Syn*Hb (a control analogous to that of $His^{hx}L$ *versus* $His^{hx}A$ RHb1 described above). The values of $K_{3,Im}$ and $K_{2,Im}$ for *Syn*Hb:$His^{hx}A$ were 93 mM^{-1} and 10 mM^{-1}, with a ratio of $K_{3,Im}/K_{2,Im}$ equal to 9.3. The affinity values for the $His^{hx}L$ mutant (420mM^{-1} and 39mM^{-1} respectively) present a similar ratio of 11 (Table 3.2). Again, the specific His^{hx} substitution affects the absolute values of $K_{3,Im}$ and $K_{2,Im}$ but not their ratio.

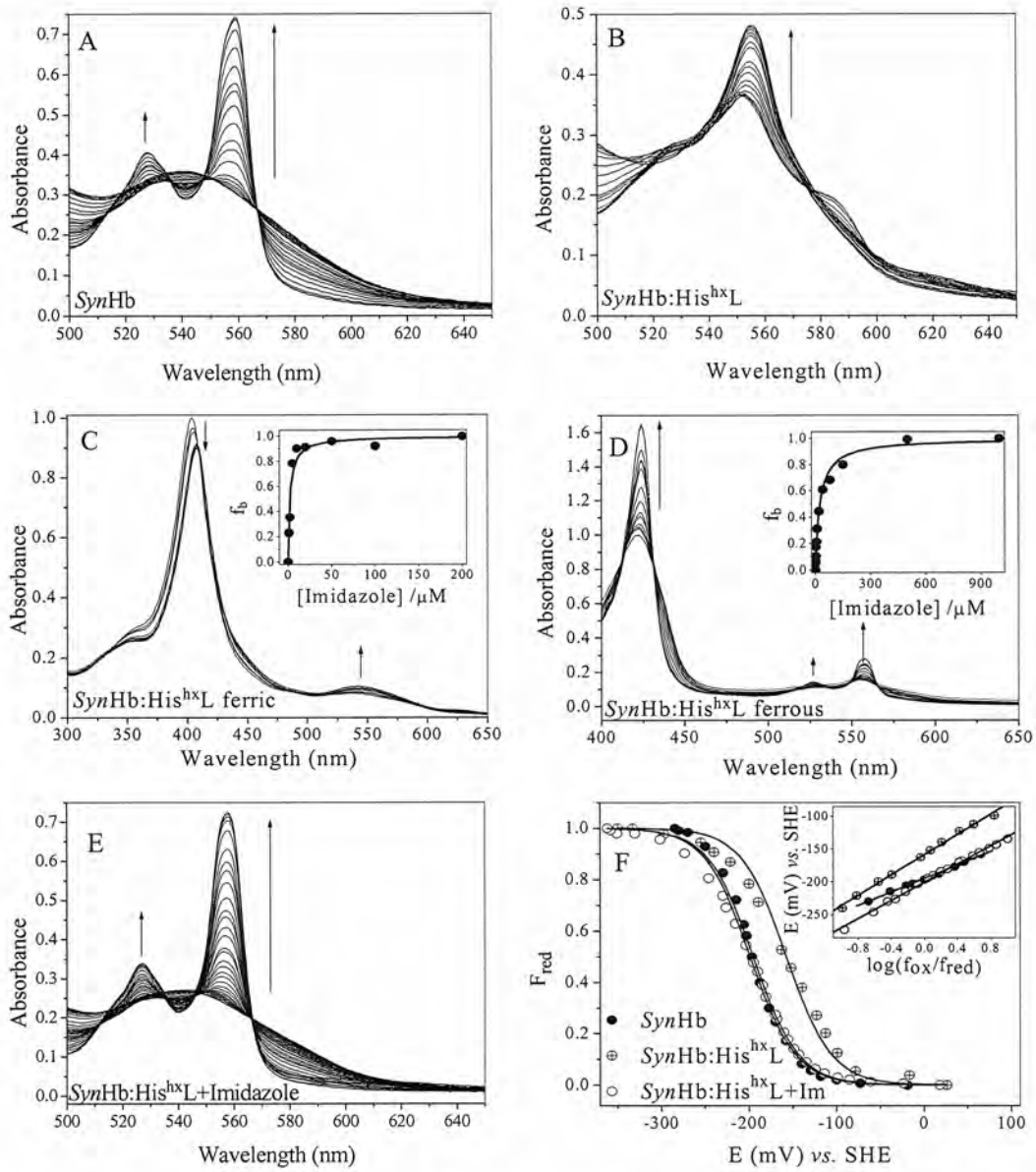

Figure 3.4 Reactions with *Syn*Hb. Spectroelectrochemical titrations of *Syn*Hb **(A)** and *Syn*Hb:His^{hx}L **(B).** Equilibrium imidazole binding to *Syn*Hb:His^{hx}L in the ferric **(C)** and ferrous **(D)** oxidation states. The insets of C and D show the fitted curve for F_B as a function of imidazole concentration. **(E)** Spectroelectrochemical titrations of *Syn*Hb:His^{hx}L saturated with imidazole (1 mM). **(F)** The fraction of reduced protein (F_{red}) in each spectroelectrochemical titration as a function of E. Solid lines show the sigmoidal fit to Equation 2.6 with E_{mid} as the fitted parameter. The inset in F represents Nernst plots of E *versus* log (F_{ox}/F_{red}), with solid lines showing linear fits.

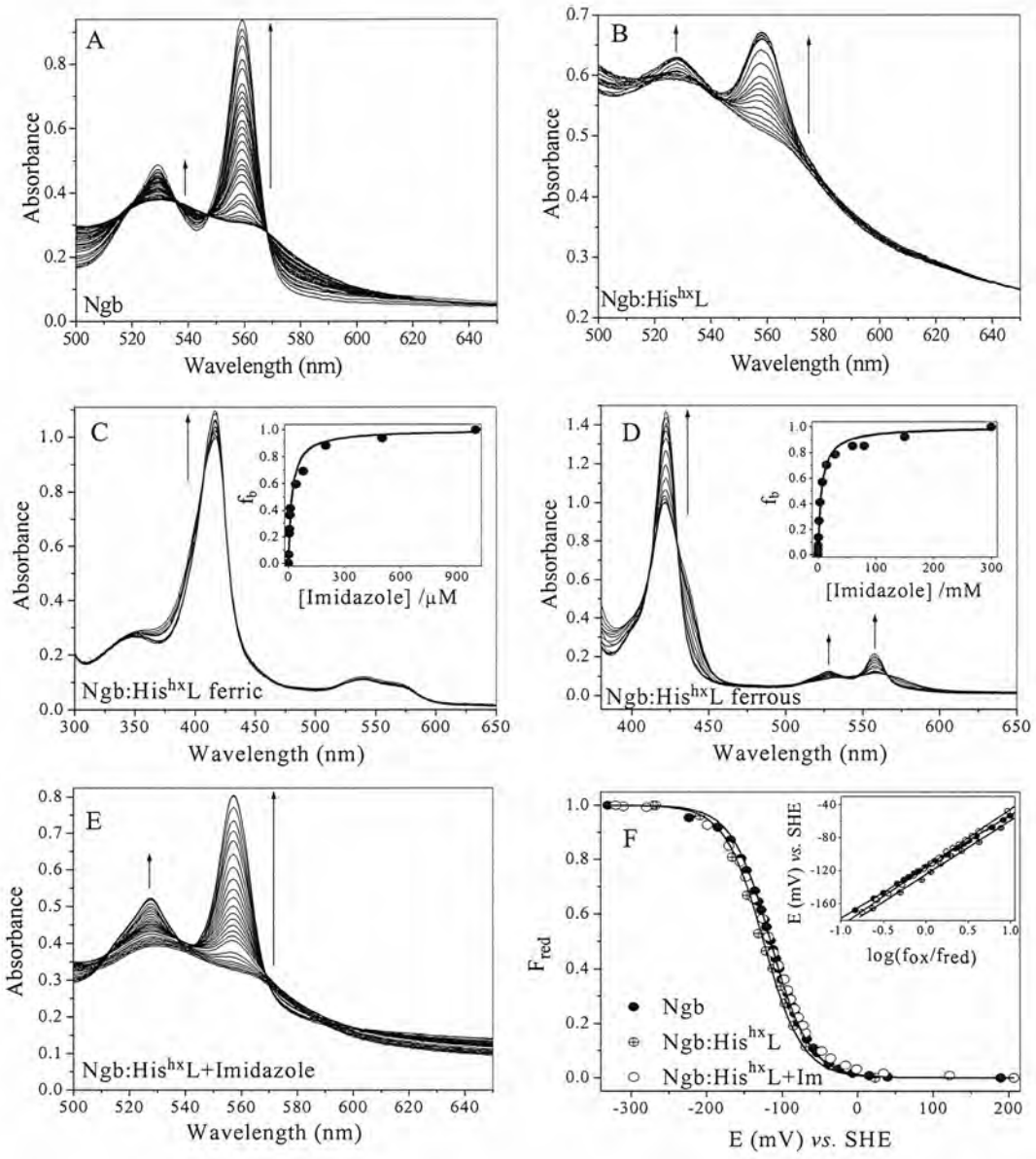

Figure 3.5 Reactions with Ngb. Spectroelectrochemical titrations of Ngb **(A)** and Ngb:His^{hx}L **(B).** Equilibrium imidazole binding to Ngb:His^{hx}L in the ferric **(C)** and ferrous **(D)** oxidation states. The insets of C and D show the fitted curve for F_B as a function of imidazole concentration. **(E)** Spectroelectrochemical titrations of Ngb:His^{hx}L saturated with imidazole (300 mM). **(F)** The fraction of reduced protein (F_{red}) in each spectroelectrochemical titration as a function of E. Solid lines show the sigmoidal fit to Equation 2.6 with E_{mid} as the fitted parameter. The inset in F represents Nernst plots of E *versus* $\log(F_{ox}/F_{red})$, with solid lines showing linear fits.

Discussion

This study presents our investigation of the role of the protein matrix in modulating the relative hexacoordination affinity constants in the ferric and ferrous oxidation states of several hxHbs. The values of $(1+K_{H3})/(1+K_{H2})$ listed in Table 3.1 provide a measure of the relative affinity constants for His^{hx} coordination in the wild-type proteins, and the values of $K_{3,Im}/K_{2,Im}$ in Table 3.2 give a measure of the relative affinity for the imidazole side chain when it is not attached to the protein matrix. A comparison of these two values, called the "affinity ratio", describes the role of the protein matrix in regulating His^{hx} binding in the different oxidation states.

One of the goals of this work was to determine if hxHbs behave in a common manner with respect to their regulation of hexacoordination. We have found that they do not. RHb1 and Cgb, which are pentacoordinate when their respective His^{hx} side chains are removed, have somewhat similar behavior in that attachment of imidazole to the protein decreases its affinity in the ferric *versus* the ferrous oxidation states. On the other hand, the Ngb and *Syn*Hb globins do not regulate hexacoordination differentially in different oxidation states.

Consequences for ligand binding in hxHbs

Perhaps a more fundamental observation results from values of $(1+K_{H3})/(1+K_{H2})$ for each hxHb. In all cases hexacoordination is tighter in the ferric oxidation state than the ferrous, but the range of affinity constant ratios is large (from 325 to 11). The significance of this value comes from its prediction of the likelihood of ferric ligand binding. Larger values of $(1+K_{H3})/(1+K_{H2})$ mean that hexacoordination presents a greater degree of competition for exogenous ligand binding in the ferric oxidation state (*50*). Proteins like

Ngb and Cgb, in which K_{H2} is already a large number (*50*), are likely to have very low affinities for ferric ligands. *Syn*Hb (which has a lower value of $(1+K_{H3})/(1+K_{H2})$) and RHb1 (which has a lower starting value of K_{H2}) would be more effective at binding ferric ligands.

The extraordinary feature of all the hxHbs investigated here is illustrated by comparison to a Mb mutant protein (H64V/V68H) that was engineered to exhibit *bis*-histidyl heme coordination (*25*). H64V/V68H Mb is relatively inert towards both ferric and ferrous ligands, indicating an inability to adopt a stable "open" conformation favorable for exogenous ligand binding. The reduction potential of H64V/V68H Mb is 204 mV lower than the corresponding pentacoordinate Mb mutant H64V (*23*) (Table 3.1). The calculated value of $(1+K_{H3})/(1+K_{H2})$ for H64V/V68H Mb is 2,800, which is significantly larger than any of the hxHbs investigated here. The ability of hxHbs to bind exogenous ligands results from their pliant protein folds, suggesting that conformational flexibility might curb tight ferric His^{hx} binding.

The role of hexacoordination in hxHbs

The preponderance of evidence supports the hypothesis that hxHbs bind exogenous ligands as part of their physiological functions (*4, 11, 51-53*). It is unlikely that hexacoordination exists solely as a mechanism to regulate ligand affinity, because large variations in binding can be achieved within the framework of a pentacoordinate fold (*12*). It is more likely that reversible hexacoordination facilitates chemistry at the active site, as might be required for enzymatic activity or associated redox reactions (*43*), or ensures a structural change that could facilitate signal transduction (*44*). In either case, a secondary

role in regulating affinity for substrate or signal would naturally result from competition of His^{hx} for the ligand binding site.

In RHb1 and Cgb, the protein matrix functions to reduce coordination of His^{hx} in the ferric state, thus enhancing the tendency of the protein to bind exogenous ferric ligands. In *Syn*Hb and Ngb, there is no disproportionate enhancement of coordination. The grouping of these pairs of hxHbs are also observed in that the RHb1 and Cgb $His^{hx}L$ mutant proteins are pentacoordinate, but those of *Syn*Hb and Ngb are not (apparently due to solvent coordination in both oxidation states). The structural features that hinder solvent coordination in RHb1:$His^{hx}L$ and Cgb:$His^{hx}L$ are possibly the same that destabilize ferric His^{hx} coordination. These results suggest that RHb1 and Cgb could share a common function involving ferric ligand binding. Additionally, the active sites of *Syn*Hb and Ngb are similar in the absence of His^{hx} coordination, suggesting a potentially common function for these two hxHbs.

The ubiquitous presence of hxHbs in living organisms implies that although their physiological roles remain obscure, they are likely to be significant. The nearly identical amino acid sequences among orthologous hxHbs also suggest they are exquisitely adapted to their function. In contrast to the rigidity, this mutational intolerance would seem to impose, the attributes associated with hexacoordination show remarkable variation. Previous studies have demonstrated a wide range of ligand binding affinities associated with hexacoordination modulation of kinetic behavior. Our results reveal that not only is heme coordination itself differentially tuned among hxHbs in general, but that the means of regulation varies among these proteins. The surprising flexibility in biophysical traits

conferred by hexacoordination suggests that they may well be capable of multiple function roles.

CHAPTER 4: CO BINDING STUDIES OF HEXACOORDINATE HEMOGLOBINS

Introduction

A basic understanding of the ligand binding phenomenon for hxHbs is necessary to judge their potential roles in vivo. The conventional kinetic techniques like flash photolysis and rapid mixing experiments have been used to study the ligand binding kinetics in HxHbs (*4, 37*). These techniques are limited due to multiphasic time courses for ligand binding (oxygen or carbon monoxide), which precludes determination of equilibrium constants from kinetic values. For this reason, different binding constants have been reported for some hxHbs which depend on how the reactions are initiated or on what time scales the data are analyzed (*4, 31, 37*).

On the contrary, for the pentacoordinate hemoglobins, ligand binding is shown to be monophasic and determination of the bimolecular rate constants does not depend on the nature of techniques employed. Due to this simplicity in ligand binding behavior the kinetic constants as well as the equilibrium constants of the ligands can be evaluated with much confidence for pentacoordinate Hbs unlike hexacoordinate ones. So, for hxHbs, a unique method for ligand binding studies needs to be developed which could surmount the limitations of the techniques used earlier. Electrochemistry is a well known technique which has been used in the past for axial ligand binding studies of heme proteins. The advantages of this technique over the others include that in one experiment both the Fe(III) and Fe(II) equilibrium constants can be evaluated and the information on the reduction potential could also be obtained for the protein with and without the axial ligand from the same experiment (*34*). This technique is also simple due to the fact that it requires only one

set of experimental data which is sufficient to determine the equilibrium binding constant for the ligand whereas for the kinetic methods, more than one set of data are required to extract the same binding constant. However, the applications of electrochemistry are limited by the availability of the redox mediators useful for buffering the potential range required for the ligand binding study, and the stability of ligands in the presence of chemical reductants like sodium dithionite. For example, when CO is bound to the pentacoordinate Hbs (mammalian Hb or Mb), one can expect change of mid-point reduction potential to a large positive value compared to the mid-point potentials for the wild type proteins, which is a reflection of their high CO affinity. This technique may not be useful in this case due to unavailability of the redox mediators at that high positive potential range. Furthermore, ligands like oxygen and NO are destroyed by sodium dithionite, and cannot be used in these experiments.

Here we present a CO binding study of four hexacoordinate hemoglobins; rice non-symbiotic hemoglobin (RHb1); *Synechocystis* hemoglobin (*Syn*Hb); human neuroglobin (Ngb) and human cytoglobin (Cgb). This study involves the measurement of the mid-point reduction potentials of the aforesaid proteins in absence and presence of different concentrations of CO. Difference in mid-point potential values can be utilized to calculate the equilibrium binding constants. These values are in good agreement with the equilibrium constants evaluated by the kinetic methods (*1, 50*).

Results

The goal of the binding experiments is to measure the equilibrium binding constants of hxHbs for CO in general, and to complement the same type of measurements

accomplished by conventional kinetic methods. The measurement of CO affinity constants by electrochemical technique requires the mid-point reduction potential of hxHb in absence of CO, which is referred as, $E_{mid,hex}$; and the mid-point potential of the same protein with a known concentration of CO, which is referred as, $E_{mid,CO}$ (Scheme 4.1) . The affinity constants of hxHbs for CO in the ferrous oxidation state of iron (CO does not bind the ferric proteins) is measured by comparing the two mid-point potentials of the proteins ($E_{mid,hex}$ and $E_{mid,CO}$).

Thermodynamic relationship between CO binding and reduction potentials

Binding of CO to wild type hxHbs is thermodynamically related with the reduction potentials of the proteins in presence and absence of CO (Scheme 4.1).

$$Hb_{ox} + e^- \overset{E_{mid,hex}}{\rightleftharpoons} Hb_{red}$$

$$Hb_{red} + CO \overset{K'_{CO}}{\rightleftharpoons} Hb_{red}CO$$

Net reaction $\Rightarrow$ $Hb_{ox} + CO + e^- \overset{E_{mid,CO}}{\rightleftharpoons} Hb_{red}CO$

Scheme 4.1 Reactions associated with CO binding and the reduction potentials of hxHbs. Hb_{ox} is the oxidized and Hb_{red} is the reduced form of the hexacoordinate protein. The exogenous ligand, CO binds with the ferrous oxidation state of the protein with an equilibrium affinity constant of K'_{CO}.

The effect of exogenous CO ligation on the mid-point potential of Hbs can be described by the following equation:

$$E_{mid,CO} = E_{mid,hex} + \frac{RT}{nF}\ln(1 + K'_{CO}[CO]) \qquad \text{Equation 4.1}$$

Rearranging the above equation, the simple relationship relating the change in potentials and concentration of CO can be obtained with the assumption of $K'_{CO}[CO] >> 1$.

$$\Delta E_{mid} \cdot \frac{nF}{RT} = \ln K'_{CO} + \ln[CO] \qquad \text{Equation 4.2}$$

Equation 4.2 shows that the difference in reduction mid-point potentials for the wild type proteins in the presence and absence of CO should increase with increasing CO concentration.

CO binding to RHb1, *Syn*Hb, Ngb, Cgb

Figure 4.1 (A to D) represents the spectral changes associated with 100μM CO binding for RHb1, *Syn*Hb, Ngb and Cgb respectively.

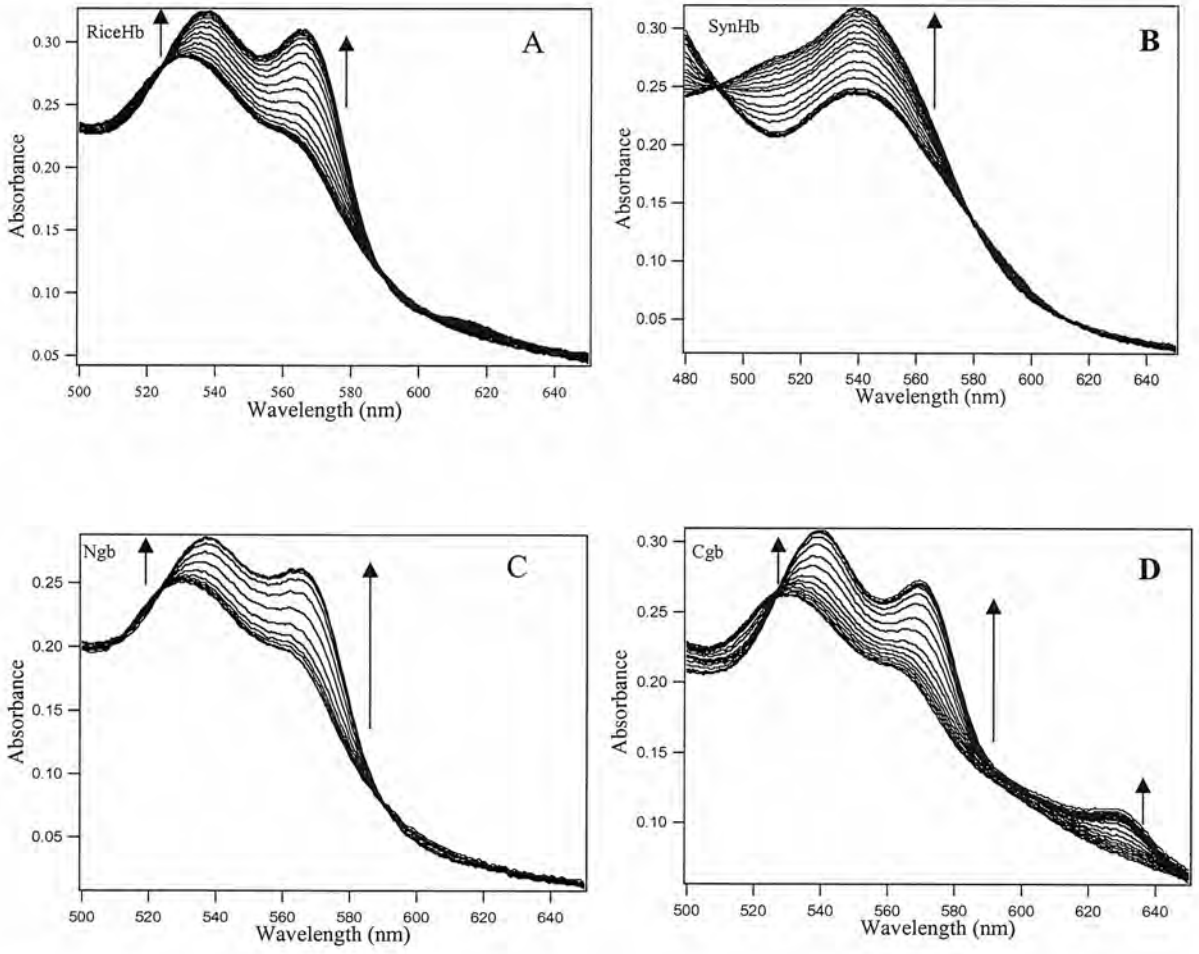

Figure 4.1 Spectral changes associated with a typical CO binding electrochemical experiments for RHb1(A), *Syn*Hb (B), Ngb(C), Cgb(D) with 100μM CO.

The Ferrous-CO spectra of RHb1, Ngb, Cgb look similar having multiple peaks in the visible region whereas *Syn*Hb shows an atypical single ferrous-CO peak around 540nm. Plots of fraction of reduced protein for four diffferent concentrations of CO (100, 50, 10, 5μM) *versus* observed potentials (E) are shown in Figure 4.2 (A to D).

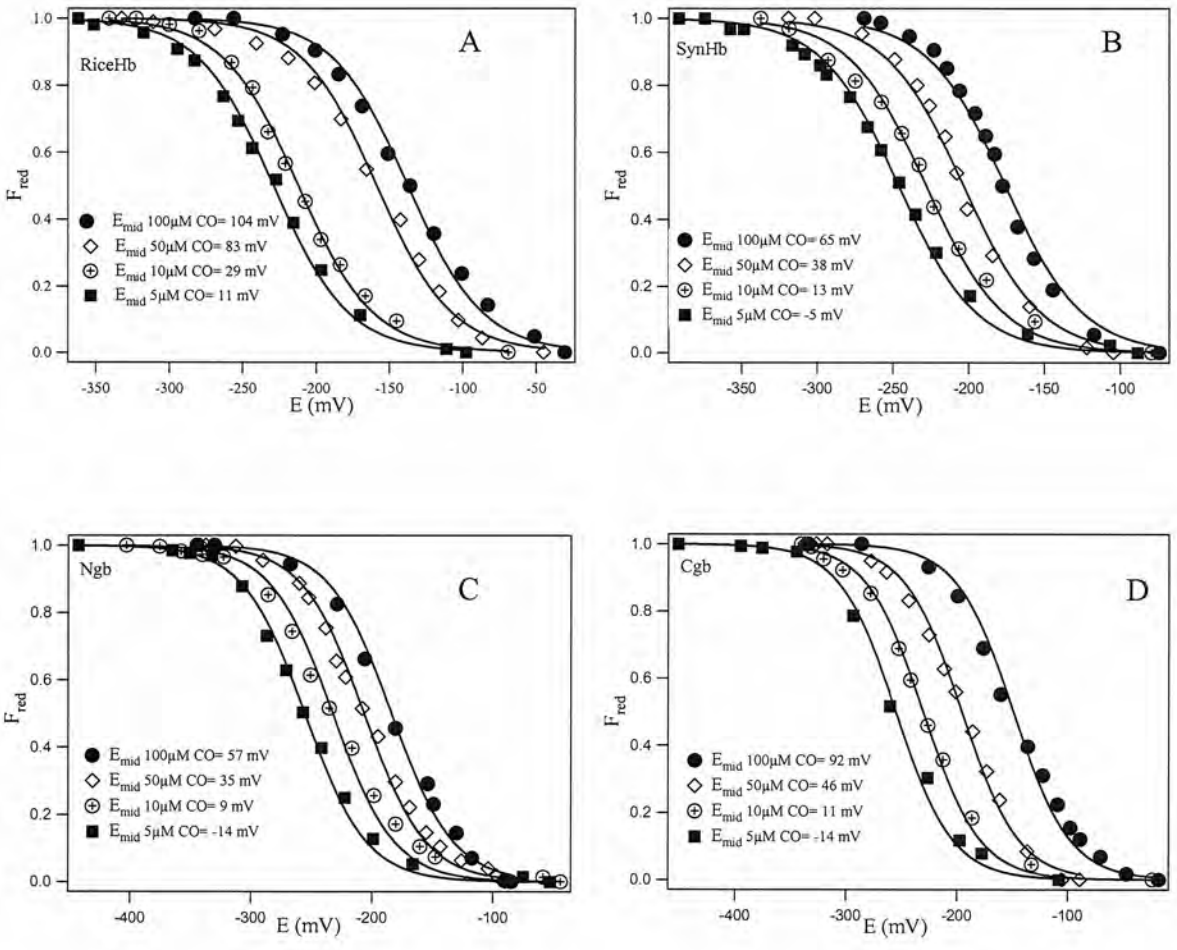

Figure 4.2 The fraction of reduced protein (F_{red}) in electrochemical titration with variable CO concentrations (100, 50, 10, 5μM) as a function of observed potentials (E) for RHb1 (A), *Syn*Hb (B), Ngb(C) and Cgb(D). Solid lines show the sigmoidal fit to equation 2.6 with $E_{mid,CO}$ as the fitted parameter at different CO concentrations.

Fits of these data to equation 2.6 yield different mid-point potential values for different proteins with their respective CO concentrations. All of these mid-point potential values are reported in Table 4.1. Figure 4.3 shows the CO concentration dependence of change in mid-point potentials for hxHbs. As disscussed in equation 4.2, from the plot of the change in mid-point potentials multiplied by (nF/RT) as a function of ln[CO], one can calculate the equilibrium affinity constant of each protein from the intercept and slope of the linear fit would be near unity.

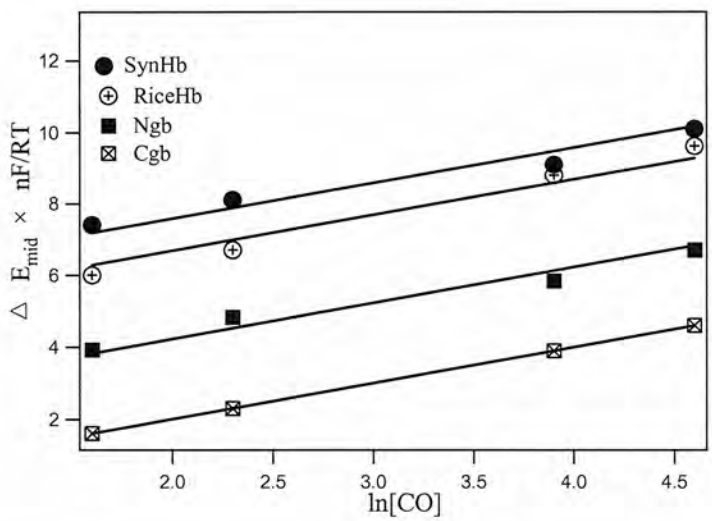

Figure 4.3 The CO concentration dependence of the change in mid-point potentials for hxHbs. Solid lines show the linear fit of $\triangle E_{mid(CO\text{-}hex)}$ as a function of ln[CO] with slopes fixed to unity.

Table 4.1 reports the equlibrium affinity constants for CO of hxHbs determined by the electrochemical method along with the reported mid-point potentials.

Table 4.1 Reduction mid-point potentials for wild type hxHbs with and without CO and comparison of the equilibrium affinity constants from electrochemical and kinetic study

Protein	$E_{mid,he}$ [a]	$E_{mid,CO}$ (100μM)	$E_{mid,CO}$ (50μM)	$E_{mid,CO}$ (10μM)	$E_{mid,CO}$ (5μM)	lnK'_{CO} [b]	K'_{CO} (E.Chem) μM^{-1}	K'_{CO} [c] (Kinetics) μM^{-1}
RHb1	-0.143	0.104	0.083	0.029	0.011	4.68	107	2300
*Syn*Hb	-0.195	0.065	0.038	0.013	-0.005	5.57	262	150
Ngb	-0.115	0.057	0.035	0.009	-0.014	2.22	9.2	5.7
Cgb	-0.028	0.092	0.046	0.011	-0.014	0.0025	1	2.2

[a]All the potentials are reported vs. standard hydrogen electrode (SHE) in V and the measured potential values lie within an error limit of ±0.005 V
[b]These values are obtained from the intercept of the plot of change in mid-point potentials as a function of ln[CO] for hxHbs (Figure 4.3)
[c]These values are calculated from Equation 4.6

The CO binding studies of His^{hx} mutants are attempted to perform in the same way as that of the wt proteins. The purpose of these experiments is that the mutants with a non-coordinating side chain (Leu) in place of distal histidine could serve as the pentacoordinate analogs of the wild type proteins and the affinity constants determined by potentiometric titration could be compared with that obtained for their wild type hexacoordinate variety. But, the CO ligation effect of ferric mutant proteins could not be investigated further due to some unusual event of reduction in presence of CO.

The reduction driven under a CO atmosphere in the absence of other added reductants (like dithionite etc.), has been referred to as "autoreduction" (*38*). They observed that cytochrome *c* oxidase and oxygen binding proteins like hemoglobin and

myoglobin in their ferric state become slowly reduced in presence of CO. They also studied the half life of this reduction reaction driven by CO for various heme proteins and found that cytochrome *c* oxidase was reduced much faster($t_{1/2}$ cyt a_3: 0.5 hr $t_{1/2}$ cyt *a*: 6 hr) than the oxidized α and β chains of human hemoglobin($t_{1/2}$ HbA 1000 hrs) and sperm whale myoglobin ($t_{1/2}$ 1200 hrs). The similar type of reductive reaction is noticed for the ferric mutant proteins of hxHbs for the first time in this study by observing their spectral changes in presence of CO which are shown in Figure 4.4, where 'A' represents the spectral study investigated in a CO atmosphere for the pentacoordinate horse heart myoglobin in ferric state and 'B' represents the spectral changes associated with the CO driven reduction phenomenon of ferric Cgb:His^{hx}L.

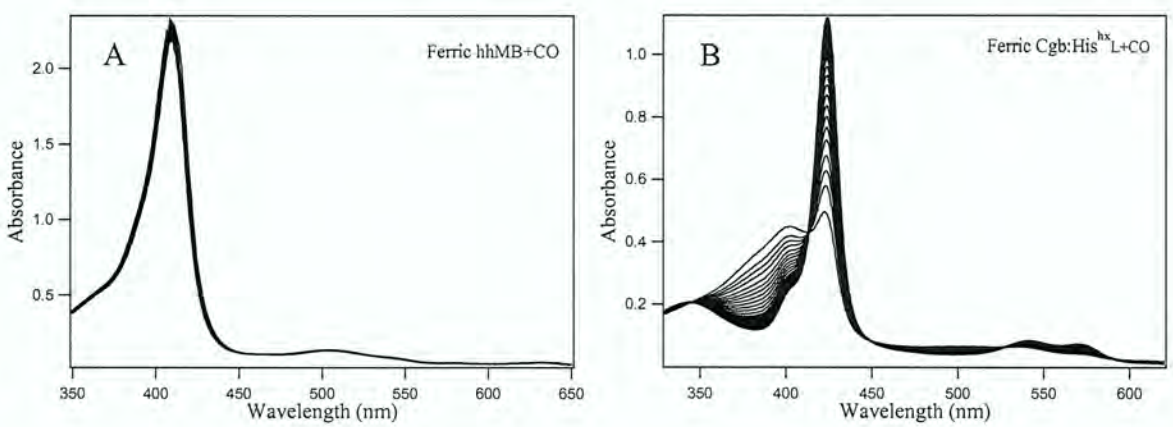

Figure 4.4 Spectral changes observed in presence of CO for ferric hhMb (A) and ferric Cgb:His^{hx}L (B)

Ferric hhMb does not show any significant change in spectral behavior with CO (Fig. 4.4 A) as also observed by Bickar and coworkers (*38*), but on the contrary, ferric Cgb:His^{hx}L shows the spectral changes characteristic of the CO-induced autoreduction (Fig. 4.4 B).

Spectral changes of the ferric $His^{hx}L$ mutants of other hxHbs are also observed under CO atmosphere. Rates of autoreduction are found to be faster for $His^{hx}L$ mutants of Cgb and Ngb compared to RHb1 and *Syn*Hb mutants (data not shown). It is also found that wild type hxHbs do not show any spectral changes in presence of CO unlike the mutants.

Discussion

Scientific studies in past few years have led not only to the discoveries of hxHbs but also their great diversity and existence in bacteria, plants, and animals. The present work is undertaken in order to get a clear scenario of the ligand binding in hxHbs as a class and to re-evaluate the importance of a relatively old electrochemical technique from a new perspective in determining their ligand affinity.

The concept of equilibrium affinity constants has been developed in the context of Hbs from their ability to bind oxygen and other potential ligands. The relationship between fraction of ligand bound protein and concentration of ligand in non-cooperative pentacoordinate Hb is given by the following equation with K'_L as the equlibrium affinity constant and $K'_L = 1/K_d = k'_L/k_L$.

$$f_B = \frac{K'_L[L]}{1 + K'_L[L]} \qquad \text{Equation 4.3}$$

The distinguishing feature of hxHbs from the pentacoordinate Hbs with respect to ligand binding comes into play because of the fact that intramolecular hexacoordination plays a crucial role in competing with the exogenous ligands which must be taken into account during the calculation of the equlibrium affinity constants. The mechanism of ligand binding for hxHbs is as follows

$$Hb_H \underset{k_H}{\overset{k_{-H}}{\rightleftarrows}} Hb_P + L \underset{k_L}{\overset{k'_L}{\rightleftarrows}} Hb_L \qquad \text{Equation 4.4}$$

In the above equation , Hb_H and Hb_P are the hexacoordinate and pentacoordinate forms of the protein, L is the exogenous ligand, k'_L is the bimolecular association, and k_L is the dissociation rate constant of the ligand. The equilibrium affinity of hxHbs, K'_L, is directly affected by the equilibrium constant for hexacoordination, K_H (*1*). Equation 4.3 will be modified by considering the hexacoordination effect , where $K_H=k_H/k_{-H}$.

$$f_B = \frac{\frac{K'_L}{1+K_H}[L]}{1+\frac{K'_L}{1+K_H}[L]} \qquad \text{Equation 4.5}$$

The effective affinity constant for hxhbs according to Equation 4.5 becomes

$$K'_{L,H} = \frac{K'_L}{1+K_H} \qquad \text{Equation 4.6}$$

Equation 4.6 indicates that hexacocordination competes with the exogenous ligand binding by reducing its affinity for the protein and the magnitude of K_H regulates the degree of reduction in $K'_{L,H}$ value for these proteins.

Measurement of equilibrium affinity for exogenous ligands of hxHbs requires the values of at least four independent kinetic constants (k'_L, k_L, k_H and k_{-H}). Recently, the binding of CO to hxHbs is reevaluated and a better model of understanding the ligand binding mechanism has been developed following rapid mixing and flash photolysis techniques (*50*). The values of k'_{CO}, k_H, k_{-H} from (*50*) and the CO dissociation rate constants (k_{CO}) from (*1*) are incorporated in equation 4.6 to determine the CO affinity values for hxHbs.

Calculation of the equlibrium affinity of hxHbs for CO by spectroelectrochemical method is mentioned in the result section of this chapter. Table 4.1 reports the calculated affinity constant values for the set of hxHbs studied here. The affinity of the wild type hxHbs for CO are found to be 260 , 9.2, 1, 107 μM^{-1} for *Syn*Hb, Ngb, Cgb and RHb1 respectively. These values are in well agreement with that obtained by the kinetic methods (Table 4.1) for most of the proteins except RHb1, which shows a significant deviation from the affinity obtained with kinetic methods. The CO affinity values for *Syn*Hb, Ngb and Cgb fall within 1-2 folds determined by two different methods but that for RHb1 measured by kinetic method differs from electrochemical technique by more than 10 fold (Table 4.1). The reason for that could be a possible error in any one of the four measured kinetic constants required to calculate the affinity for this protein (Equation 4.6). Other proteins show a good correlation of the affinity for CO determined by two different methods.

The CO-driven reduction reaction of ferric His^{hx} mutant proteins draws special attention because it is somewhat unusual. The mechanism of reduction is not clear. Bickar and coworkers (*38*) suggeted that CO catalyzes the reduction of ferric heme proteins by the following mechanism

$$Fe(III) + CO + H_2O \rightarrow CO_2 + 2H^+ + Fe(II) \qquad \text{Equation 4.7}$$

The detailed mechanism underlying this observation is still not understood. But it is known that the Hb-CO derivatives are much more stable with respect to the oxy or deoxy form of the proteins. Since the reduced hemoglobin is much more stable than the oxidized form, the reductive process under CO would tend to improve the stability of the protein. A similar reductive reaction of methemyoglobin is also observed after binding with NO. Brudvig and coworkers (*54*) observed that cytochrome a_3 becomes reduced under an

atmosphere of NO. This reductive reaction in presence of CO or in some cases for NO might have some physiological significance. The detailed study of this CO-driven reactions in His^{hx} mutants for hxHbs needs to be done in this regard.

CHAPTER 5: CONCLUSION AND FUTURE DIRECTIONS

Significance of redox potentials in the context of heme proteins

The tendency of a redox couple to donate or accept electrons is given by its redox potential (E). The value 'E' exhibited by an individual couple is a reflection of the relative stability of the reduced and oxidized states. Any factor which tends to stabilize the oxidized form makes the redox couple a better electron donor and results in a more negative redox potential, whereas the factor that stabilizes the reduced form would make it a better electron acceptor and a more positive potential will be observed. These effects can be utilized to determine the alterations in the free energy levels of the oxidized and reduced species (G_{ox} and G_{red}). Although the determination of the absolute values of G_{ox} and G_{red} are not possible out of the electrochemical measurements, information about the change in free energy ($\triangle G_{stab}$, free energy of stabilization) can be calculated in terms of change in redox potential ($\triangle E$) by the following equation

$$\Delta G_{stab} = -nF\Delta E \qquad \text{Equation 5.1}$$

This $\triangle G_{stab}$ is a measure of the ease of electron transfer in a particular direction for a redox pair. The higher the change in potentials ($\triangle E$) in the positive direction thus lowering of the change in free energy ($\triangle G_{stab}$), the higher will be the tendency for the system to be reduced.

The free energy of stabilization ($\triangle G_{stab}$) is a composite term (*40*)

$$\Delta G_{stab} = \Delta G^{lig} + \Delta G^{coord} + \Delta G^{el} + \Delta G^{conf} \qquad \text{Equation 5.2}$$

$\triangle G^{lig}$ is the stabilization effect achieved by binding of a ligand to the protein; $\triangle G^{coord}$ is conferred due to the coordination characteristic of the protein at the redox center;

$\triangle G^{el}$ considers the electrostatic interactions between the charges at the redox center and the charges within the protein matrix in its vicinity or the polar solvent; $\triangle G^{conf}$ is the conformational stabilization energy. An assessment of the individual components of $\triangle G_{stab}$ is possible as long as the other terms in equation 5.2 remain constant.

With the development of site directed mutagenesis, the coordination character of the proteins could be altered with the same overall three dimensional structures and the same type of active site and thus the direct impact on their redox potential can be easily evaluated (*34*). The purpose of the study presented in chapter 3 of this thesis is based upon the above fact. The results demonstrated here could be used to extract the free energy of stabilization manifested mainly due to the coordination effect of hxHbs at the heme center ($\triangle G^{coord}$) described in equation 5.2. In this chapter, the effect of alteration of the coordination behavior of hxHbs is being examined in general. Another strong point in favor of the study is to explore how this coordination behavior is influenced by the different protein matrices for different hxHbs and finally to answer the question whether they have any similarity in their mode of action which might be related to their potential physiological functions. The results show significant variation among the hxHbs, demonstrating flexibility in the globin moiety's ability to regulate reversible coordination. This regulation is primarily evident in plant nsHb where ferric state intramolecular His affinity is substantially lowered by the protein matrix; Cgb shows moderate regulation and the protein matrices for *Syn*Hb and Ngb do not differentially control the coordination behavior.

The focus of chapter 4 experiments is to study the ligand binding effect on redox potential of hxHbs based on the treatment of Moore and Pettigrew according to reaction

scheme 7.2, and the results might be related with ($\triangle G^{lig}$) term of equation 5.2. It was shown (*40*) that the mid-point potential in absence of ligand for a redox protein is modified by a factor containing redox-state dependent dissociation constants and the relevant ligand concentration. We have used the same set of equations to obtain the alteration of mid-point potential of hxHbs depending on the ligand (CO) concentration, except we have plugged in the association equilibrium constant (alternatively, ligand affinity) in all of our calculations instead of using the dissociation equilibrium constants. The results reveal the affinity of hxHbs with CO as exogenous ligand with a great deal of accuracy and their absolute values corroborate well with the affinity determined from the kinetic methods.

Future applications of SEC technique

The principal technique which was adopted for the entire ligand binding process and also for studying the coordination behavior of hxHbs is called Spectroelectrochemistry (SEC). This technique has potential for investigating the redox proteins in variety of ways from the effect of mutagenesis related with the alteration of coordination feature or change of electrostatic environment around the active site to different ligand binding phenomenon. Being a direct method, this is especially useful to explore the structure and function of this new class of hexacoordinate hemoglobins in details.

Future work involving this technique could include the extensive mutagenesis study of hxHbs revealing the importance of other amino acid residues which are not directly related with the coordination nature of the protein but play crucial roles in modifying heme reactivity in different ways. SEC also has future applicability with respect to the binding of other physiologically important ligands (e.g.; NO) with hxHbs. It is speculated that hxHbs

could serve as the NO scavenger in plants and animals so a thorough understanding of NO binding to these proteins needs to be developed.

References

1. Trent, J. T., III, Watts, R. A., and Hargrove, M. S. (2001) *J. Biol. Chem. 276*, 30106-30110.
2. Trent, J. T., III, and Hargrove, M. S. (2002) *J. Biol. Chem. 277*, 19538-19545.
3. Hargrove, M. S., Brucker, E. A., Stec, B., Sarath, G., Arredondo-Peter, R., Klucas, R. V., Olson, J. S., and Phillips, J., George N. (2000) *Structure 8*, 1005-1014.
4. Trent, J. T., III, Hvitved, A. N., and Hargrove, M. S. (2001) *Biochemistry 40*, 6155-6163.
5. Couture, M., Das, T. K., Savard, P.-Y., Ouellet, Y., Wittenberg, J. B., Wittenberg, B. A., Rousseau, D. L., and Guertin, M. (2000) *Eur J Biochem 267*, 4770-4780.
6. Pesce, A., Couture, M., Dewilde, S., Guertin, M., Yamauchi, K., Ascenzi, P., Moens, L., and Bolognesi, M. (2000) *EMBO J. 19*, 2424-2434.
7. Burmester, T., Ebner, B., Weich, B., and Hankeln, T. (2002) *Mol Biol Evol 19*, 416-421.
8. Burmester, T., and Hankeln, T. (2004) *News Physiol Sci 19*, 110-113.
9. Hamdane, D., Kiger, L., Dewilde, S., Green, B. N., Pesce, A., Uzan, J., Burmester, T., Hankeln, T., Bolognesi, M., Moens, L., and Marden, M. C. (2003) *J. Biol. Chem. 278*, 51713-51721.
10. Arredondo-Peter, R., Hargrove, M. S., Sarath, G., Moran, J. F., Lohrman, J., Olson, J. S., and Klucas, R. V. (1997) *Plant Physiol. 115*, 1259-1266.
11. Dordas, C., Rivoal, J., and Hill, R. D. (2003) *Ann Bot (Lond) 91 Spec No*, 173-8.
12. Kundu, S., Trent, J. T., III, and Hargrove, M. S. (2003) *Trends in Plant Science 8*, 387-393.

13. Hankeln, T., Ebner, B., Fuchs, C., Gerlach, F., Haberkamp, M., Laufs, T. L., Roesner, A., Schmidt, M., Weich, B., and Wystub, S. (2005) *Journal of Inorganic Biochemistry 99*, 110-119.

14. Ortiz de Montellano, P. R. (1987) *Acc. Chem. Res. 20*, 289-294.

15. Raphael, A. L., and Gray, H. B. (1989) *Proteins: Struct.,Funct., Genet. 6*, 338-340.

16. Raphael, A. L., and Gray, H. B. (1991) *J. Am. Chem. Soc. 113*, 1038-1040.

17. Rodriguez, J. C., and Rivera, M. (1998) *Biochemistry 37*, 13082-13090.

18. Adachi, S., Nagano, S., Watanabe, Y., Ishimori, K., and Morishima, I. (1991) *Biochem. Biophys. Res. Commun. 180*, 138-144.

19. Adachi, S., Nagano, S., Ishimori, K., Watanabe, Y., Morishima, I., Egawa, T., Kitagawa, T., and Makino, R. (1993) *Biochemistry 32*, 241-252.

20. Lloyd, E., Hildebrand, D. P., Tu, K. M., and Mauk, A. G. (1995) *J. Am. Chem. Soc. 117*, 6434-6438.

21. Barker, P. D., Nerou, E. P., Cheesman, M. R., Thomson, A. J., Oliveira, P., and Hill, H. A. O. (1996) *Biochemistry 35*, 13618-13626.

22. Barrick, D. (1994) *Biochemistry 33*, 6546-6554.

23. Van Dyke, B. R., Saltman, P., and Armstrong, F. A. (1996) *J. Am. Chem. Soc. 118*, 3490-3492.

24. Varadarajan, R., Zewert, T. E., Gray, H. B., and Boxer, S. G. (1989) *Science 243*, 69-72.

25. Dou, Y., Admiraal, S. J., Ikeda-Saito, M., Krzywda, S., Wilkinson, A. J., Li, T., Olson, J. S., Prince, R. C., Pickering, I. J., and George, G. N. (1995) *J. Biol. Chem. 270*, 15993-16001.

26. Jones, D. K., Patel, N., and Raven, E. L. (2002) *Arch.Biochem.Biophys. 400*, 111-117.

27. Taniguchi, V. T., Ellis, W. R. J., Cammarata, V., Webb, J., Anson, F. C., and Gray, H. B. (1982) *Adv.Chem.Ser 201*, 51-68.

28. Oritz de Montellano, P. R., and Catalano, C. E. (1985) *J.Biol.Chem 260*, 9265-9271.

29. Huang, Y. Y., Hara, T., Silgar, S., Coon, M. J., and Kimura, T. (1986) *Biochemistry 25*, 1390-1394.

30. Reid, L. S., Taniguchi, V. T., Gray, H. B., and Mauk, A. G. (1982) *J Am Chem Soc 104*, 7516-7519.

31. Dewilde, S., Kiger, L., Burmester, T., Hankeln, T., Baudin-Creuza, V., Aerts, T., Marden, M. C., Caubergs, R., and Moens, L. (2001) *J. Biol. Chem. 276*, 38949-38955.

32. Lecomte, J. T., Scott, N. L., Vu, B. C., and Falzone, C. J. (2001) *Biochemistry 40*, 6541-52.

33. Sawai, H., Kawada, N., Yoshizato, K., Nakajima, H., Aono, S., and shiro, Y. (2003) *Biochemistry 42*, 5133-5142.

34. Nesset, M. J. M., Shokhirev, N. V., Enemark, P. D., Jacobson, S. E., and Walker, F. A. (1996) *Inorg. Chem. 35*, 5188-5200.

35. Halder, P., Trent, J. T., III, and Hargrove, M. S. (2006) *Submitted.*

36. Nienhaus, K., Kriegl, J. M., and Nienhaus, G. U. (2004) *J. Biol. Chem. 279*, 22944-22952.

37. Hvitved, A. N., Trent, J. T., III, Premer, S. A., and Hargrove, M. S. (2001) *J. Biol. Chem. 276*, 34714-34721.

38. Bickar, D., Bonaventura, C., and Bonaventura, J. (1984) *J.Biol.Chem 259*, 10777-10783.

39. Altuve, A., Wang, L., Benson, D. R., and Rivera, M. (2004) *Biochem. Biophys. Res. Commun. 314*, 602-609.

40. Moore, G., and Pettigrew, G. (1990) *Springer series in molecular biology, Springer, Berlin, New York.*

41. Bogumil, R., Hunter, C. L., Maurus, R., Tang, H. L., Lee, H., Lloyd, E., Brayer, G. D., Smith, M., and Mauk, A. G. (1994) *Biochemistry 33*, 7600-8.

42. Lloyd, E., King, B. C., Hawkridge, F. M., and Mauk, A. G. (1998) *Inorg. Chem. 37*, 2788-2892.

43. Weiland, T. R., Kundu, S., Trent, J. T., III, Hoy, J. A., and Hargrove, M. S. (2004) *J Am Chem Soc 126*, 11930-5.

44. Trent, J. T., III, Kundu, S., Hoy, J. A., and Hargrove, M. S. (2004) *Journal of Molecular Biology 341*, 1097-1108.

45. Mauk, A. G., and Moore, G. R. (1997) *Journal of Inorganic Biochemistry 2*, 119–125.

46. Hildebrand, D. P., Burk, D. L., Maurus, R., Ferrer, J. C., Brayer, G. D., and Mauk, A. G. (1995) *Biochemistry 34*, 1997-2005.

47. Patel, N., Seward, H. E., Svensson, A., Gurman, S. J., Thomson, A. J., and Raven, E. L. (2003) *Arch Biochem Biophys 418*, 197-204.

48. Kundu, S., Snyder, B., Das, K., Chowdhury, P., Park, J., Petrich, J. W., and Hargrove, M. S. (2002) *Proteins 46*, 268-77.

49. Olson, J. S., and Phillips, G. N., Jr. (1996) *J Biol Chem 271*, 17593-6.

50. Smagghe, B. J., Sarath, G., Ross, E., Hilbert, J. L., and Hargrove, M. S. (2006) *Biochemistry 45*, 561-70.

51. Kundu, S., Premer, S. A., Hoy, J. A., Trent, J. T., III, and Hargrove, M. S. (2003) *Biophys. J. 84*, 3931-3940.

52. Hargrove, M. S. (2000) *Biophys. J. 79*, 2733-2738.

53. Arredondo-Peter, R., Hargrove, M. S., Moran, J. F., Sarath, G., and Klucas, R. V. (1998) *Plant Physiol 118*, 1121-5.

54. Brudvig, B., Stevens, T., and Chan, S. (1980) *Biochemistry 19*, 5275-5285.

Acknowledgements

I would like to express deep appreciation to my research advisor, Dr. Mark Hargrove, for his guidance, support, knowledge and assistance throughout this endeavor. I would also like to thank Dr. Mario Rivera, Dr. David Benson and Adriana Altuve for advice on constructing our electrochemical titration apparatus. Thanks are also due to all past and present fellow members of Hargrove lab for their friendship and support.

I am thankful to my parents for their love and support to keep me up. I would also like to take the opportunity to thank all of my family members for their constant encouragements. Last but not the least; I would like to thank my husband for providing me everything needed to make my life happy.